METABOLISM OF ORGANOSULFUR COMPOUNDS IN *RUEGERIA POMEROYI* DSS-3

by

WARREN CRABB

(Under the Direction of William B. Whitman)

ABSTRACT

Dimethylsulfoniopropionate (DMSP) accounts for up to 10% of the carbon fixed by marine phytoplankton, most of which, is released as dissolved organic matter available for degradation and assimilation by bacterioplankton. Bacterial metabolism of DMSP proceeds via two competing pathways: demethylation or cleavage. The latter releases dimethyl sulfide (DMS), a climatically relevant gas and a major source of atmospheric sulfur. The demethylation pathway was found to be highly abundant in marine bacteria and accounts for a majority of DMSP degradation. In addition to being a source of energy and sulfur for marine bacteria, the demethylation pathway directs transformation of DMSP away from formation of DMS. A number of techniques were utilized to elucidate the pathways and enzymology of DMSP metabolism in the marine bacteria, *Ruegeria pomeroyi* DSS-3.

INDEX WORDS: Dimethylsulfoniopropionate; DMSP; Methanethiol; MeSH; Acrylate; 3-Hydroxypropionate; Metabolism; Assimilation; Sulfur; Ruegeria pomeroyi

METABOLISM OF ORGANOSULFUR COMPOUNDS IN *RUEGERIA POMEROYI* DSS-3

by

WARREN CRABB
B.S, Armstrong Atlantic State University, 2010

A Thesis Submitted to the Graduate Faculty of The University of Georgia in Partial Fulfillment of the Requirements for the Degree

MASTER OF SCIENCE

ATHENS, GEORGIA
2013

METABOLISM OF ORGANOSULFUR COMPOUNDS IN *RUEGERIA POMEROYI* DSS-3

by

WARREN CRABB

Major Professor:	William B. Whitman
Committee:	Mary Ann Moran
	Robert J. Maier

Electronic Version Approved:

Maureen Grasso
Dean of the Graduate School
The University of Georgia
August 2013

ACKNOWLEDGEMENTS

I would like to acknowledge the generous support and mentorship given by my thesis advisor Dr. William B. Whitman. I would also like to acknowledge Dr. Mary Ann Moran for her support and limitless enthusiasm as well as Dr. Robert Maier for his help and guidance. Finally, I would like to thank the members of the Whitman lab for their support and friendship.

TABLE OF CONTENTS

Page

LIST OF TABLES

Page

LIST OF FIGURES

Page

CHAPTER 1

Literature Review

The ubiquitous phytoplankton metabolite dimethylsulfoniopropionate (DMSP) is a major source of reduced sulfur and carbon for marine microbes. The concentration of dissolved DMSP ranges from less than 1 nM up to 50 nM in surface waters with intracellular concentrations reaching 1.0 M in some phytoplankton [14]. DMSP accounts for up to 10% of the carbon fixed by marine phytoplankton, where it functions primarily as an osmoprotectant [23] with proposed secondary roles as an antioxidant [33], predator deterrent [44], and cryoprotectant [15]. Much of the interest in DMSP stems from the hypothesis that it is a precursor for the climatically active gas dimethyl sulfide (DMS) [25]. Oxidation of atmospheric DMS results in the formation of sulfate, sulfur dioxide, and other sulfur gases that may act as cloud condensation nuclei, thus increasing solar backscatter and effectively lowering the amount of solar radiation reaching the ocean surface. Therefore, the release of DMS acts as a negative feedback loop by decreasing phytoplankton growth and reducing DMSP production (Figure 1). This hypothesis, referred to as CLAW for the surnames of authors who proposed it, has recently been called into question [29]. Regardless of the impact of DMS on cloud formation, it still remains a significant source of gaseous sulfur to the marine troposphere [2]. It is estimated that 40 Teragrams/year of DMS are released from marine systems globally from non-anthropogenic sources, where it accounts for 42% of the atmospheric sulfur burden [32].

While some DMSP is degraded by the marine algae that synthesized it, most of the 12-100 Tmol DMSP-S released each year from phytoplankton is accumulated and metabolized by

marine bacteria through two competing pathways (Figure 2). Referred to as the demethylation and cleavage pathways, these pathways result in the release of methanethiol (MeSH) or DMS, respectively. By examining size, fractionation, and chemical fate of [^{35}S]DMSP incubations, Vila-Costa *et al.* [43] estimated 10–50% of DMSP synthesized from algae is released as dissolved matter. The estimated fates of the sulfur from this released DMSP were 20–40% transformation to nonvolatile sulfur (DMSO, sulfate or other compounds), 5–30% assimilation by bacteria into the protein fraction, and 2–5% transformation to DMS.

Using incubations of oceanic and coastal waters amended with ^{35}S radiolabeled DMS, MeSH and DMSP, Kiene and Linn [21] measured the end product partitioning of the sulfur moiety (Figure 3). Approximately 15% of the ^{35}S accumulated intracellularly, was found as un-degraded DMSP. This pool of DMSP reached concentrations of roughly 70 mM and is hypothesized to function as an osmoprotectant [30]. In coastal waters nearly 60% of the [^{35}S]DMSP was incorporated into cellular material, possibly into methionine via assimilation of MeSH. In contrast, only 16% was incorporated in oceanic waters. The higher assimilation rates of DMSP sulfur in coastal waters is likely due to increased growth rates; suggesting a higher sulfur demand for organisms inhabiting these systems. MeSH that was not incorporated was oxidized to nonvolatile dissolved sulfur. DMS turnover was much lower than the flux from DMSP to MeSH. Small amounts of the sulfur from DMS were converted to cell protein, but most of it was converted to sulfate.

Following incubations of coastal and oceanic samples with [^{35}S]DMS, 70% of DMS was converted to DMSO, 3% was incorporated into macromolecules, and the remainder was oxidized to SO_2^- [43]. Samples pre-incubated with DMS formed less DMSO. The authors speculate that there was a population of bacteria, perhaps in the roseobacter clade or a *Hypomicrobium,* that

converts DMS to MeSH and then to HS^- by heterotrophic oxidation of the methyl groups. This HS can then be oxidized to SO_2^-. In total, up to 90% of the DMSP sulfur enters the demethylation pathway, forming MeSH, which is then incorporated into cells or degraded to sulfate. Of the DMSP that is cleaved to DMS, 60–99% of the sulfur in DMS is not released, being transformed to sulfate or DMSO. [43]

DMSP Demethylation

The model organism *Ruegeria pomeroyi* (formerly *Silicibacter*) is capable of metabolizing DMSP through either the demethylation or cleavage pathway (Figure 2). *dmdA, the* gene responsible for initiating demethylation of DMSP, was identified in 2006 by transposon mutagenesis [14]. Subsequent characterization revealed that it encodes a tetrahydrofolate (THF)-dependent enzyme that produces 5-methyl-THF and methylmercaptopropionate (MMPA) [30]. Homologues to *R. pomeroyi dmdA* are abundant in genomic databases, and the discovery of a homologue in the ubiquitous SAR11 clade bacterium *Pelagibacter ubique* solidified the importance of DMSP demethylation in the global carbon and sulfur cycles.

Most of the MMPA produced by DMSP demethylation is ultimately converted to MeSH, CO_2, and acetaldehyde through a series of coenzyme-A (CoA) mediated reactions [31]. Like *dmdA,* the genes involved in the next two steps of MMPA catabolism *(dmdB* and *dmdC)* are abundant in marine surface waters. Analysis of the GOS metagenomic dataset suggests that *dmdB* and *dmdC* are present in 61% of marine bacteria [27]. Interestingly, homologues to these genes are widely distributed in non-marine bacteria such as *Myxococcus xanthus*, *Burkholderia* spp., and *Deinococcus* [31], indicating that some steps in the demethylation pathway may play a wider role than initially thought. In contrast to the abundance of *dmdB* and *dmdC* homologues,

the final gene in the pathway, *dmdD*, is relatively rare with only 16 homologues identified in the GOS compared to the 6,200 of *dmdB* and *dmdC*. Recently, a non-orthologous isofunctional enzyme (DmdD') has been identified in *Ruegeria lacuscaerulensis* that may provide clues to the 'missing' enzymes in the GOS dataset.

MeSH incorporation and utilization

As seen above, a significant percent of sulfur derived from DMSP is first converted to MeSH and ultimately assimilated by bacteria. However, the route by which MeSH is assimilated is poorly understood. One possibility is that the entire MeSH molecule is incorporated into methionine. The enzyme cystathionine γ-synthase (EC 2.5.1.48) is thought to be responsible for this activity [19]. The typical function of this enzyme is to catalyze the release of succinate from O-succinyl-L-homoserine and stimulate the formation of a C-S bond between cysteine and homoserine to form cystathionine. This enzyme, however, has broad substrate specificity. When methanethiol is the substrate instead of cysteine, it will form a C-S bond between methanethiol and homoserine to form methionine [10]. The sulfur in methanethiol is at the same redox state as the sulfur in methionine; as such, this reaction would allow the conservation of reducing equivalents during the synthesis of methionine. Moreover, DMSP was found to be an essential source of reduced sulfur in *P. ubique* and, by extension, the highly abundant SAR11 clade; thus, direct assimilation of MeSH by this reaction may be an obligatory method of methionine synthesis [40].

A second possible fate of MeSH is complete oxidation to sulfide. MeSH may be used as a source of energy by autotrophic thiobacilli and diverse methyl-oxidizing aerobic bacteria and by methylotrophic hyphomicrobia as a source of carbon and energy [3; 6; 16]. MeSH is degraded in

Hyphomicrobium and *Thiobacillus* by methanethiol oxidase (E.C. number 1.8.3.4), producing formaldehyde and sulfide by the following reaction: methanethiol + O_2 + H_2O → formaldehyde + H_2S + H_2O_2. The enzyme that catalyzes this reaction was purified from *Rhodococcus rhodochrous* [22], but no genes encoding this function are known.

DMSP Cleavage

Ruegeria pomeroyi expresses three enzymes, DddP, DddQ, and DddW, capable of cleaving DMSP to DMS and acrylate [37; 38; 39]. A mutation in *dddQ* reduces DMS production by 95% in *R. pomeroyi*, suggesting that this is the dominant enzyme under certain conditions [40]. In comparison to wild-type *R. pomeroyi,* DddP and DddW mutants decrease DMS production by 55% and 50%, respectively. All three enzymes share predicted structural similarity in the form of a cupin-binding domain, but lack significant sequence similarity.

Three additional DMSP cleavage enzymes have been identified in addition to the enzymes shown to have physiological activity in *R. pomeroyi.* The first, DddD, was shown to produce 3-hydroxypropionate instead of acrylate [35; 36]. *dddD* negative *R. pomeroyi* produced wild-type levels of DMS under standard growth conditions. The role of DddD in this organism remains unclear. The gene encoding DddL was identified in a cosmid library of *Sulfitobacter* sp. EE-36, and a *dddL* deletion mutant was unable to produce DMS from DMSP [5]. DddY was first purified and characterized in 1995 from a marine isolate *Alcaligenes faecalis* M3A. However, only recently was the gene encoding this enzyme identified [4]. DddY has no homology to the other DMSP lyases.

In contrast to the genes encoding steps involved in the demethylation pathway, the genes encoding the cleavage pathway are less abundant in the GOS metagenome database [31]. *dddP*,

the most widespread of the DMSP lyases is present in approximately 6% of marine bacteria. The remaining known DMSP lyases are present at <0.5%. The low abundance of these genes may be one contributing factor for the observed lower flux of DMSP to DMS in environmental samples (Fig. 3).

Significant progress has been made to elucidate the biochemical pathways by which DMSP is degraded; however, the biological factors that control which pathway is utilized are effectively unknown. The work being carried out in our lab will attempt to shed new light on the environmental and physiological conditions that regulate these pathways.

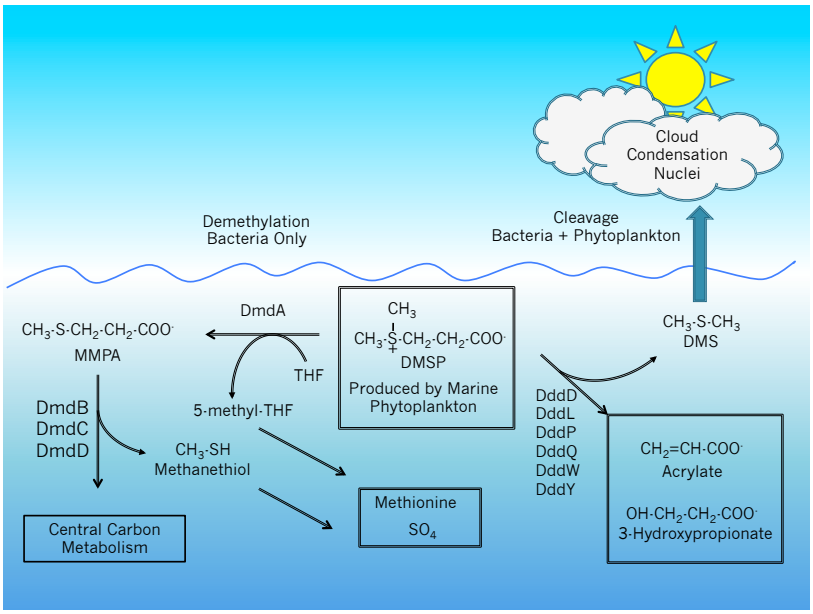

Figure 1.1 Overview of DMSP degradation pathways in the marine environment

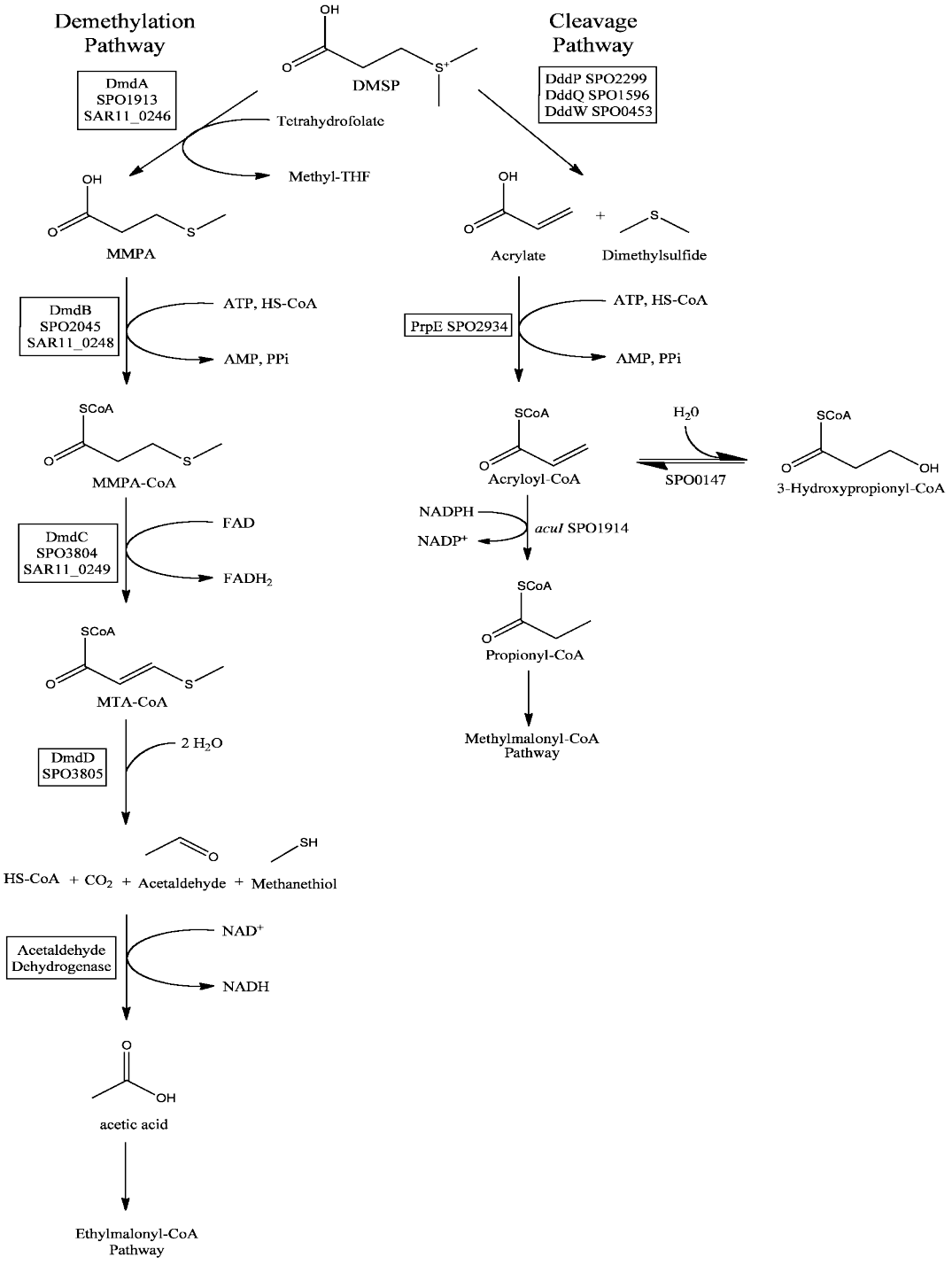

Figure 1.2 Pathways of DMSP metabolism in *Ruegeria pomeroyi* DSS-3

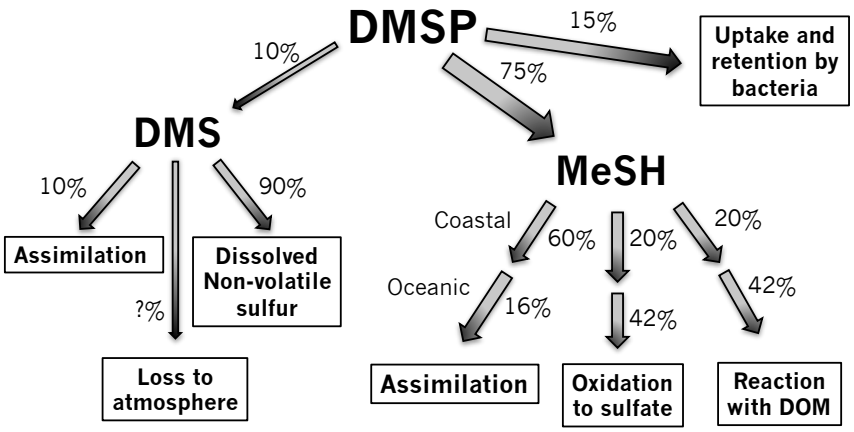

Figure 1.3 End point partition of sulfur moiety derived from DMSP. Adapted from ref. 21

1.4 References

[1] **Bürgmann, H., E. C. Howard, W. Ye, F. Sun, S. Sun, S. Napierala, and M. A. Moran.** 2007. Transcriptional response of silicibacter pomeroyi dss-3 to dimethylsulfoniopropionate (dmsp). *Environ Microbiol*, 9(11):2742–55, 11

[2] **Covert, D. S., Kapustin, V. N., Quinn, P. K., & Bates, T. S.** 1992. New particle formation in the marine boundary layer. *Journal of Geophysical Research D*, 97, 20581–20589.

[3] **Bentley, R. and T. G. Chasteen**. 2004. Environmental VOSCs–formation and degradation of dimethyl sulfide, methanethiol and related materials. *Chemosphere*, 55:291–317.

[4] **Curson, A. R., M. J. Sullivan, J. D. Todd, and A. W. Johnston.** 2011. DddY, a periplasmic dimethylsulfoniopropionate lyase found in taxonomically diverse species of Proteobacteria. ISME J.

[5] **Curson, A. R. J., R. Rogers, J. D. Todd, C. A. Brearley, and A. W. B. Johnston.** 2008. Molecular genetic analysis of a dimethylsulfoniopropionate lyase that liberates the climate-changing gas dimethylsulfide in several marine alpha-proteobacteria and *Rhodobacter sphaeroides*. Environ Microbiol 10:1099-1099.

[6] **de Zwart, J. M. M. and J. G. Kuenen.** 1992. C1-cycle of sulfur compounds. *Biodegradation*, 3:37–59.

[7] **Dias, B. and B. Weimer.** 1998. Purification and characterization of l-methionine gamma-lyase from brevibacterium linens bl2. *Applied and environmental microbiology*, 64(9):3327,

[8] **Erb, T.J., G. Fuchs, and B.E. Alber.** 2009. (2s)-methylsuccinyl-coa dehydrogenase closes the ethylmalonyl-coa pathway for acetyl-coa assimilation. *Molecular microbiology*, 73(6):992–1008.

[9] **Erb, T. J., I. A. Berg, V. Brecht, M. Müller, G. Fuchs, and B. E. Alber.** 2007. Synthesis of c5-dicarboxylic acids from c2-units involving crotonyl-coa carboxylase/reductase: the ethylmalonyl-coa pathway. *Proc Natl Acad Sci U S A*, 104(25):10631–6, 6.

[10] **Flavin, M. and C. Slaughter.** 1967. Enzymatic synthesis of homocysteine or methionine directly from O-succinyl-homoserine. *Biochimica et Biophysica Acta*, 132:400–5.

[11] **González, J. M., R. P. Kiene, and M. A. Moran.** 1999. Transformation of sulfur compounds by an abundant lineage of marine bacteria in the alpha-subclass of the class proteobacteria. *Appl Environ Microbiol*, 65(9):3810–9, 9.

[12] **Gould, W. D. and T. Kanagawa.** 1992. Purification and properties of methyl mercaptan oxidase from thiobacillus thioparus tk-m. *Journal of General Microbiology*, 138(1):217.

[13] **Henriksen, J. R. H**., 2008. Physiology of Dimethylsulfoniopropionate Metabolism in a Model Marine Roseobacter*, Silicibacter pomeroyi*. PhD thesis, The University of Georgia.

[14] **Howard, E. C. , J. R Henriksen, A. Buchan, C. R. Reisch, H. Bürgmann, R. Welsh, W. Ye, J. M. González, K. Mace, S. B. Joye, R. P. Kiene, W. B. Whitman, and M. A. Moran.** 2006. Bacterial taxa that limit sulfur flux from the ocean. *Science*, 314(5799):649–52, 10.

[15] **Karsten, U., K. Kuck, C. Vogt, and G.O. Kirst.** 1996. Dimethylsulfoniopropionate production in phototrophic organisms and its physiological function as a cryoprotectant. *Biological and environmental chemistry of DMSP and related sulfonium compounds. Plenum Press, New York*, pages 143–153.

[16] **Kelly, D. P. and S. C. Baker.** 1990. The organosulphur cycle: aerobic and anaerobic processes leading to turnover of C1-sulphur compounds. *FEMS Microbiology Letters*, 87:241–246.

[17] **Kerr, D.S.** 1971. O-acetylhomoserine sulfhydrylase from neurospora. *Journal of Biological Chemistry*, 246(1):95,

[18] **Kiene, R. P.**1996. Production of methanethiol from dimethylsulfoniopropionate in marine surface waters. *Marine chemistry*, 54(1-2):69–83.

[19] **Kiene, R. P., L. J. Linn, J. González, M. A. Moran, and J. A. Bruton.** 1999. Dimethylsulfoniopropionate and methanethiol are important precursors of methionine and protein-sulfur in marine bacterioplankton. *Appl Environ Microbiol*, 65(10):4549–58, 10.

[20] **Kiene, R. P., & Linn, L. J.** 2000. The fate of dissolved dimethylsulfoniopropionate (DMSP) in seawater: Tracer studies using 35S-DMSP. *Geochimica Et Cosmochimica Acta*, *64*(16), 2797-2810.

[21] **Kiene, R. P. and L. J. Linn**. 2000b. The fate of dissolved dimethylsulfoniopropionate (DMSP) in seawater: tracer studies using 35S-DMSP. *Geochimica et Cosmochimica Acta*, 64:2797–2810

[22] **Kim, S. J., H. J. Shin, Y. C. Kim, D. S. Lee, and J. W. Yang.** 2000. Isolation and purification of methyl mercaptan oxidase from rhodococcus rhodochrous for mercaptan detection. *Biotechnology and Bioprocess Engineering*, 5(6):465–468.

[23] **Kirst, G. O.** 1996. Osmotic adjustment in phytoplankton and macroalgae: the use of dimethylsulfoniopropionate (dmsp). *Biological and environmental chemistry of DMSP and related sulfonium compounds. Plenum Press, New York, NY*, pages 121–129.

[24] **Liu, Y., W.B. Whitman, and R.H. White.** 2010. Cysteine is not the sulfur source for iron-sulfur cluster and methionine biosynthesis in the methanogenic archaeon methanococcus maripaludis. *Journal of Biological Chemistry*, 285(42):31923.

[25] **Lovelock, J. E., R. J. Maggs, and R. A. Rasmussen.** 1972. Atmospheric dimethyl sulphide and the natural sulphur cycle. *Nature*, 237(5356):452–453.

[26] **McAllan, D.T, T.V. Cullum, R. A. Dean, and F. A. Fidler.** 1951. The preparation and properties of sulfur compounds related to petroleum. The dialkyl sulfides and disulfides. *Journal of the American Chemical Society*, 73(8):3627–3632.

[27] **Moran, M. A., C. R. Reisch, R. P. Kiene, and W. B. Whitman.** 2012. Genomic Insights into Bacterial DMSP

Transformations. Annu Rev Mar Sci 4

[28] **Murooka, Y., K. Kakihara, T. Miwa, K. Seto, and T. Harada.** 1977. O-alkylhomoserine synthesis catalyzed by o-acetylhomoserine sulfhydrylase in microorganisms. *Journal of Bacteriology*, 130(1):62.

[29] **Quinn, P.K. and Bates, T.S.** 2011. The case against climate regulation via oceanic phytoplankton sulphur emissions. *Nature,* 480(7375):51-56.

[30] **Reisch, C. R., Mary Ann Moran, and William B. Whitman.** 2008. Dimethylsulfoniopropionate-dependent demethylase (dmda) from pelagibacter ubique and silicibacter pomeroyi. *J Bacteriol*, 190(24):8018–24.

[31] **Reisch, C. R., M. J. Stoudemayer, V. A. Varaljay, I. J. Amster, M. A. Moran, and W. B. Whitman**. 2011. Novel pathway for assimilation of dimethylsulphoniopropionate widespread in marine bacteria. *Nature*, 473(7346):208–11.

[32] **Simó, R., C. Pedros-Alio, G. Malin, and J. O. Grimalt.** 2000. Biological turnover of DMS, DMSP and DMSO in contrasting open-sea waters. *Marine Ecology Progress Series*, 203:1–11.

[33] **Sunda, W., D. J. Kieber, R. P. Kiene, and S. Huntsman.** 2007. An antioxidant function for dmsp and dms in marine algae. *Nature*, 418(6895):317–20.

[34] **Suylen, G. M. H., P. J. Large, J. P. Van Dijken, and J. G. Kuenen.** 1987. Methyl mercaptan oxidase, a key enzyme in the metabolism of methylated sulphur compounds by hyphomicrobium eg. *Journal of general microbiology*, 133(11):2989.

[35] **Taylor, K. A.** 1997. A colorimetric formaldehyde assay. *Applied Biochemistry and Biotechnology*, *68*(1),81-93.

[36] **Todd, J. D., A. R. Curson, N. Nikolaidou-Katsaraidou, C. A. Brearley, N. J. Watmough, Y. Chan, P. C.**

Page, L. Sun, and A. W. Johnston. 2010. Molecular dissection of bacterial acrylate catabolism - unexpected links with dimethylsulfoniopropionate catabolism and dimethyl sulfide production. Environ Microbiol. 12:327-343.

[37] **Todd, J. D., R. Rogers, Y. G. Li, M. Wexler, P. L. Bond, L. Sun, A. R. Curson, G. Malin, M. Steinke, and**

A. W. Johnston. 2007. Structural and regulatory genes required to make the gas dimethyl sulfide in bacteria. Science 315:666-669.

[38] **Todd, J. D., A. R. J. Curson, C. L. Dupont, P. Nicholson, and A. W. B. Johnston.** 2009. The dddp gene, encoding a novel enzyme that converts dimethylsulfoniopropionate into dimethyl sulfide, is widespread in ocean metagenomes and marine bacteria and also occurs in some ascomycete fungi. *Environmental Microbiology*, 11(6):1624–1625.

[39] **Todd, J.D., M. Kirkwood, S. Newton-Payne, and A.W.B. Johnston.** 2011. Dddw, a third dmsp lyase in a model roseobacter marine bacterium, ruegeria pomeroyi dss-3. *The ISME Journal.*

[40] **Todd, J. D., R. J. Curson, M. Kirkwood, M. J. Sullivan, R. T. Green, and A. W. B. Johnston.** 2011. Dddq, a novel, cupin-containing, dimethylsulfoniopropionate lyase in marine roseobacters and in uncultured marine bacteria. *Environ Microbiol*, 13(2):427–38.

[41] **Tripp, H. J., J. B. Kitner, M. S. Schwalbach, J. W. H. Dacey, L. J. Wilhelm, and S. J. Giovannoni**. 2008. SAR11 marine bacteria require exogenous reduced sulphur for growth. *Nature*.

[42] **van Duyl, F. C., W. W. C. Gieskes, A. J. Kop, and W. E. Lewis.** 1998. Biological control of short-term variations in the concentration of dmsp and dms during a phaeocystis spring bloom. *Journal of Sea Research*, 40(34):221–231.

[43] **Vila-Costa, M., D. A. D. Valle, J. M. González, D. Slezak, R. P. Kiene, O. Sánchez, and R. Simó** 2006. Phylogenetic identification and metabolism of marine dimethylsulfide-consuming bacteria. *Environmental Microbiology*, 8:2189–200.

[44] **Wolfe, G. V., M. Steinke, and G. O. Kirst.** 1997. Grazing-activated chemical defence in a unicellular marine

alga. *Nature*, 387(6636):894–897.

Chapter 2

Crystal structure of DmdD, a crotonase superfamily enzyme that catalyzes the hydration and hydrolysis of methylthioacryloyl-CoA

2.1 Introduction

Dimethyl-sulphoniopropionate (DMSP) is produced in abundant quantities by marine surface-water phytoplankton, including coccolithophores, dinoflagellates, and diatoms, as well as some plants common in salt marshes. In these organisms, the compound plays a role in osmoregulation, stress control, detoxification, and other functions [1,2,3,4]. DMSP is an important source of carbon and reduced sulfur for marine bacteria. It is catabolized through two competing pathways, releasing either the climatically active gas dimethylsulphide (DMS) or the highly reactive volatile gas methanethiol (MeSH). For the DMS pathway, a lyase catalyzes the cleavage of DMSP, producing DMS and acrylate (or occasionally 3-hydroxypropionate in some bacteria). For the MeSH pathway, DMSP is first demethylated to produce 3-methylmercaptopropionate (MMPA), which is then esterified to coenzyme A (CoA). MMPA-CoA is demethiolated through a set of reactions analogous to b-oxidation of fatty acids—a dehydrogenation reaction produces methylthioacryloyl-CoA (MTA-CoA) followed by a hydration reaction that ultimately converts MMPA to acetaldehyde, CO_2, and MeSH.

The enzyme DmdD catalyzes the last step of the MeSH pathway, the hydration and hydrolysis of MTA-CoA [2]. DmdD belongs to the crotonase superfamily of enzymes, homologous to the equivalent enzyme in the fatty acid b-oxidation pathway. For example,

Ruegeria pomeroyi DmdD shares 32% amino acid sequence identity with rat liver enoyl-CoA hydratase (ECH), a canonical crotonase. Of special interest, the two acidic residues that are important for the catalysis of ECH (Glu144 and Glu164) are also conserved in DmdD (Glu121 and Glu141). Enzymes in the crotonase superfamily are mechanistically diverse and catalyze many different types of reactions on CoA esters [5], including hydration [6], hydrolysis [7,8,9,10], isomerization [11], dehalogenation [12], decarboxylation [13], and others.

To understand the molecular basis for the unique catalytic activities of DmdD, we have determined the crystal structures of *R. pomeroyi* wild-type DmdD free enzyme and the E121A mutant in complex with MTA-CoA or MMPA-CoA at 1.5, 1.8, and 1.8 Å resolution, respectively. Our structures reveal conformational differences for the C-terminal loop of DmdD compared to canonical crotonases, which affect the organization of the active site. MTA-CoA and MMPA-CoA have similar binding modes in the active site. However, MMPA-CoA cannot be hydrated and is only hydrolyzed slowly by DmdD. Replacement of the sulfur atom in MMPA-CoA with a methylene group abolishes hydrolysis, suggesting that the unique property of the substrate is a major determinant of the hydrolysis activity of DmdD.

2.2 Materials and Methods

Sources and synthesis of CoA thioesters

Butyryl-CoA, isobutyryl-CoA, malonyl-CoA, acetyl-CoA, 3-hydroxybutyryl-CoA and crotonyl-CoA were purchased from Sigma-Aldrich. MTA-CoA and MMPA-CoA were synthesized enzymatically as describe by Reisch *et. al.* [2]. Pentanoyl-CoA was prepared from the acid anhydride using the methods described by Stadtman [25]. Acryloyl-CoA was synthesized from acryloyl chloride (Sigma-Aldrich) as describe by Kuchta & Abeles [26]. CoA thioesters that

were synthesized were purified by reverse phase chromatography using an Ultrasphere ODS preparative column (10 x 250 mm). With the exception of acryloyl-CoA, the column was developed with 50 mM ammonium acetate (pH 6) and a gradient of 2-20% acetonitrile. The CoA thioesters were detected at 254 nm. Fractions containing the CoA thioester were lyophilized, re-suspended in dH_2O and again lyophilized. For acryloyl-CoA, the column was developed with 50 mM sodium phosphate (pH 7) and a gradient of 2-20% acetonitrile. The fractions containing acryloyl-CoA were then pooled and concentrated 3-4-fold under a stream of N_2 gas.

Enzyme assays and kinetic analyses

Enzyme assays were performed in 100 mM HEPES (pH 7.4) with substrate concentrations of 1, 2.5, 5.0, 10, 25, 50, and 150 μM. Reactions were initiated with the addition of enzyme, incubated for 2-10 minutes, quenched by addition of H_3PO_4, and briefly centrifuged to remove denatured proteins. Coenzyme-A release and the formation of 3-hydroxybutyryl-CoA from crotonyl-CoA were determined by HPLC using a 4.6 x 150 mm, 3 mm, Hypersil Gold column (Thermo-Fisher) developed with a linear gradient of 2-20% acetonitrile in 50 mM ammonium acetate (pH 6) over 10 min. A Waters model 2487 UV detector was used at 260 nm. 3-Hydroxybutyryl-CoA was identified by coelution with authentic standard. MeSH release was determined in sealed vials. The headspace was sampled, and MeSH was measured by gas chromatography on an SRI 8610-C gas chromatograph with a Chromosil 330 column (Supelco) with N_2 carrier gas at a flow rate of 60 ml min^{-1}, an oven temperature of 60°C, and a flame photometric detector. A standard curve for MeSH was obtained by suspending sodium methanethiolate (Sigma-Aldrich) in H_2O. The final values of MeSH produced were then calculated from the sum of the MeSH in the headspace plus the MeSH dissolved in the assay

solution. This latter value was calculated from a Henry's constant of 0.1447 at 25 °C [27]. In control experiments, the amount of MeSH produced was equal to the amount of HS-CoA detected by HPLC, indicating that MeSH was measured quantitatively.

All enzyme assays were performed with an acid-killed enzyme controls or T0, in which acid was added to the assay buffer prior to the addition of enzyme. Any observed product was then subtracted from the enzymatic rates. However, only very low rates of nonenzymatic hydration of MTA-CoA were observed. Kinetic data were analyzed using SigmaPlot 10.0 with the Enzyme Kinetics module (Systat Software Inc.).

2.3 Results and Discussion

Kinetic studies of DmdD

We characterized the catalytic activities of wild-type DmdD and the active site mutants (E121A, E141A, and E121A/E141A) toward MTA-CoA, MMPA-CoA and other CoA analogs—acryloyl-CoA, crotonyl-CoA, and pentanoyl-CoA. We monitored the hydrolysis of the CoA ester as well as the release of MeSH from MTA-CoA and MMPA-CoA. Wild-type DmdD has strong activity toward MTA-CoA, both for MeSH release (equivalent to hydration of MTA-CoA) and for CoA ester hydrolysis (Table 1). The k_{cat}/K_m value for wild-type DmdD is 5×10^6 $M^{-1}s^{-1}$, ~10-fold less than that for ECH, which is diffusion limited. This result suggests that DmdD is well adapted for MTA-CoA hydration, which is its physiological activity. In contrast, no MeSH release could be detected with the MMPA-CoA substrate, and CoA ester hydrolysis is also much weaker (~400-fold lower k_{cat}/K_m) with this substrate.

The E121A and E121A/E141A mutation abolished MeSH release and CoA ester hydrolysis activities against all the substrates tested (Table 1). Interestingly, the E141A mutant

showed very weak (~88,000-fold lower k_{cat}/K_m compared to the wild-type enzyme) but detectable MeSH release activity, although it had no CoA ester hydrolysis activity.

Crotonyl-CoA is an analog of MTA-CoA. Wild-type DmdD catalyzed the hydration of this substrate to produce 3-hydroxybutyryl-CoA, although the k_{cat} for this reaction, 42 s^{-1} (Table 1), was much lower than that of the canonical crotonases, which are in the range of 2,000-6,000 s^{-1} [16,17,18]. Although the kinetics could not be determined because of competition with the hydration reaction, DmdD also catalyzed the release of CoA from crotonyl-CoA (Fig. 1A). Moreover, DmdD catalyzed the hydrolysis of 3-hydroxylbutyryl-CoA with a k_{cat} of 13 s^{-1} (Table 1). Because these hydrolysis reactions compete with the hydration of crotonyl-CoA, it is unclear if they are part of the physiological reactions of this enzyme.

Acryloyl-CoA is one carbon shorter than crotonyl-CoA, but wild-type DmdD showed no detectable activity (hydration or CoA ester hydrolysis) toward this substrate. Pentanoyl-CoA is an isosteric analog of MMPA-CoA, with the replacement of the sulfur atom of MMPA by a methylene group. However, wild-type DmdD and the mutants displayed no detectable CoA ester hydrolysis activity toward this substrate. Likewise, we did not observe any hydrolysis activity for wild-type DmdD against acetyl-CoA, malonyl-CoA, butyryl-CoA, and isobutyryl-CoA either.

Catalytic mechanism of DmdD

Our studies show that DmdD catalyzes the efficient hydration as well as hydrolysis of MTA-CoA. The hydration reaction is analogous to the canonical crotonase enzymes, and likely employs a similar mechanism, with Glu121 as the general base and Glu141 as the general acid (Fig. 2). The MeSH release activity of DmdD is a spontaneous outcome after the hydration of

MTA-CoA, and does not require enzymatic catalysis. This is also supported by the fact that DmdD cannot release MeSH from MMPA-CoA.

Hydroxycinnamoyl-CoA hydratase-lyase (HCHL) is another crotonase that possesses CoA ester hydrolysis activity [7]. The enzyme proceeds through an anhydride mechanism, where an active site carboxylate group attacks the carbonyl carbon of the CoA ester. This produces an enzyme-substrate anhydride, which is then hydrolyzed by a solvent water molecule. Besides the anhydride mechanism, an elimination-addition mechanism has also been observed for the hydrolysis of CoA esters [19]. This involves the abstraction of the a proton of the CoA ester, which gives rise to an enolate. Elimination of CoA produces a ketene intermediate, which is followed by the addition of a hydroxide to generate the acid product. Finally, hydrolysis of the CoA ester by the enzyme CarB most likely proceeds through the attack of the carbonyl carbon by a water molecule activated by an active site glutamate side chain [9].

For DmdD, the Glu141 residue either directly attacks the carbonyl carbon of the CoA ester (the anhydride mechanism) or activates a water molecule for the attack to catalyze CoA ester hydrolysis (Fig. 2). This is supported by our observation that the E141A mutant has weak hydration activity (MeSH release) but no hydrolysis activity (Table 1). At the same time, the strongest hydrolysis activity is observed for MTA-CoA, while MMPA-CoA and crotonyl-CoA are hydrolyzed at much lower rates and pentanoyl-CoA is not hydrolyzed. Therefore, the presence of both the double bond and the sulfur atom in the substrate is important for the hydrolysis activity. MTA-CoA is converted to malonate semialdehyde-CoA after hydration and MeSH release, and the 3-aldehyde group may also be an important factor in stimulating the hydrolysis reaction.

With hydration followed by release of MeSH and hydrolysis to eliminate CoA, MTA-CoA is converted to malonyl semialdehyde by DmdD (Fig. 2). It is expected that this compound can spontaneously decompose, producing CO_2 and acetaldehyde, thereby explaining the observed products of the reaction.

2.4 References

1. **Otte ML, Wilson G, Morris JT, Moran BM** (2004) Dimethylsulphoniopropionate (DMSP) and related compounds in higher plants. J Exp Botany 55: 1919-1925.
2. **Reisch CR, Stoudemayer MJ, Varaljay VA, Amster IJ, Moran MA, et al.** (2011) Novel pathway for assimilation of dimethylsulphoniopropionate widespread in marine bacteria. Nature 473: 208-211.
3. **Reisch CR, Moran MA, Whitman WB** (2011) Bacterial catabolism of dimethylsulfoniopropionate. Front Microbiol 2: 172.
4. **Curson ARJ, Todd JD, Sullivan MJ, Johnston AWB** (2011) Catabolism of dimethylsulphoniopropionate: microorganisms, enzymes and genes. Nat Rev Microbiol 9: 849-859.
5. **Hamed RB, Batchelar ET, Clifton IJ, Schofield CJ** (2008) Mechanisms and structures of crotonase superfamily enzymes-how nature controls enolate and oxyanion reactivity. Cell Mol Life Sci 65: 2507-2527.
6. **Bahnson BJ, Anderson VE, Petsko GA** (2002) Structural mechanism of enoyl-CoA hydratase: three atoms from a single water are added in either an E1cb stepwise or concerted fashion. Biochem 41: 2621-2629.
7. **Wong BJ, Gerlt JA** (2003) Divergent function in the crotonase superfamily: an anhydride intermediate in the reaction catalyzed by 3-hydroxyisobutyryl-CoA hydrolase. J Amer Chem Soc 125: 12076-12077.

8. **Eberhard ED, Gerlt JA** (2004) Evolution of function in the crotonase superfamily: the stereochemical course of the reaction catalyzed by 2-ketocyclohexanecarboxyl-CoA hydrolase. J Amer Chem Soc 126: 7188-7189.

9. **Batchelar ET, Hamed RB, Ducho C, Claridge TDW, Edelmann MJ, et al.** (2008) Thioester hydrolysis and C-C bond formation by carboxymethyl-proline synthase from the crotonase superfamily. Angew Chem Int Ed 47: 9322-9325.

10. **Hamed RB, Batchelar ET, Mecinovic J, Claridge TDW, Schofield CJ** (2009) Evidence that thienamycin biosynthesis proceeds via C-5 epimerization: ThnE catalyzes the formation of (2S,5S)-trans-carboxymethylproline. Chembiochem 10: 246-250.

11. **Modis Y, Filppula SA, Novikov DK, Norledge B, Hiltunen JK, et al.** (1998) The crystal structure of dienoyl-CoA isomerase at 1.5 Å resolution reveals the importance of aspartate and glutamate sidechains for catalysis. Structure 6: 957-970.

12. **Benning MM, Taylor KL, Liu R-Q, Yang G, Xiang H, et al.** (1996) Structure of 4-chlorobenzoyl coenzyme A dehalogenase determined to 1.8 Å resolution: an enzyme catalyst generated via adaptive mutation. Biochem 35: 8103-8109.

13. **Benning MM, Haller T, Gerlt JA, Holden HM** (2000) New reactions in the crotonase superfamily: Structure of methylmalonyl CoA decarboxylase from Escherichia coli. Biochem 39: 4630-4639.

14. **Holm L, Kaariainen S, Rosenstrom P, Schenkel A** (2008) Searching protein structure databases with DaliLite v.3. Bioinformatics 24: 2780-2781.

15. **Engel CK, Mathieu M, Zeelen JP, Hiltunen JK, Wierenga RK** (1996) Crystal structure of the enoyl-coenzyme A (CoA) hydratase at 2.5 Å resolution: a spiral fold defines the CoA-binding pocket. EMBO J 15: 5135-5145.

16. **Waterson RM, Hill RL** (1972) Enoyl coenzyme A hydratase (crotonase). Catalytic properties of crotonase and its possible regulatory role in fatty acid oxidation. J Biol Chem 247: 5258-5265.

17. **Kiema TR, Engel CK, Schmitz W, Filppula SA, Wierenga RK, et al.** (1999) Mutagenic and enzymological studies of the hydratase and isomerase activities of 2-enoyl-CoA hydratase-1. Biochem 38: 2991-2999.

18. **Feng Y, Hofstein HA, Zwahlen J, Tonge PJ** (2002) Effect of mutagenesis on the stereochemistry of enoyl-CoA hydratase. Biochem 41: 12883-12890.

19. **Douglas KT** (1986) Elimination-addition pathways for thiol esters. Acc Chem Res 19: 186-192.

20. **Otwinowski Z, Minor W** (1997) Processing of X-ray diffraction data collected in oscillation mode. Method Enzymol 276: 307-326.

21. **Jogl G, Tao X, Xu Y, Tong L** (2001) COMO: A program for combined molecular replacement. Acta Cryst D57: 1127-1134.

22. **Brunger AT, Adams PD, Clore GM, DeLano WL, Gros P, et al.** (1998) Crystallography & NMR System: A new software suite for macromolecular structure determination. Acta Cryst D54: 905-921.

23. **Emsley P, Cowtan KD** (2004) Coot: model-building tools for molecular graphics. Acta Cryst D60: 2126-2132.

24. **Adams PD, Grosse-Kunstleve RW, Hung L-W, Ioerger TR, McCoy AJ, et al.** (2002) PHENIX: building a new software for automated crystallographic structure determination. Acta Cryst D58: 1948-1954.

25. **Stadtman ER** (1957) Preparation and assay of acyl coenzyme-A and other thiol esters - use of hydroxylamine. Methods Enzymol 3: 931-941.

26. **Kuchta RD, Abeles RH** (1985) Lactate reduction in Clostridium propionicum. Purification and properties of lactyl-CoA dehydratase. J Biol Chem 260: 13181-13189.

27. **Staudinger J, Roberts PV** (2001) A critical compilation of Henry's law constant temperature dependence relations for organic compounds in dilute aqueous solutions. Chemosphere 44: 561-576.

Table 1.
Summary of kinetic parameters

Reaction	**Substrate**	**Wild-type DmdD**	**E121A**	**E141A**	**E121A/E141A**
K_m (mM) [1]					
CoA ester hydrolysis	MTA-CoA	8.2 ± 2.0	N.A. [2]	N.A.	N.A.
	MMPA-CoA	69.0 ± 16.4	N.A.	N.A.	N.A.
	3-hydroxybutyryl-CoA	119 ± 20			
MeSH release	MTA-CoA	9.4 ± 2.1	N.A.	63.3 ± 12.0	N.A.
	MMPA-CoA	N.A.			
Hydration	Crotonyl-CoA	19.0 ± 3.1			
k_{cat} (s^{-1}) [1]					
CoA ester hydrolysis	MTA-CoA	44 ± 4	N.A.	N.A.	N.A.
	MMPA-CoA	0.9 ± 0.1	N.A.	N.A.	N.A.
	3-hydroxybutyryl-CoA	13.2 ± 1.6			
MeSH release	MTA-CoA	47 ± 3	N.A.	0.0036 ± 0.0004	N.A.
	MMPA-CoA	N.A.			
Hydration	Crotonyl-CoA	42 ± 3			

1. Values shown are the average and standard deviation from triplicate experiments. Acetyl-CoA, acryloyl-CoA, butyryl-CoA, isobutyryl-CoA, malonyl-CoA and pentanoyl-CoA were also tried as substrates for CoA ester hydrolysis, but no activity was observed. In addition, acryloyl-CoA was not hydrated.

2. N.A. – No activity was detected. The limits for detection were 1.4×10^{-4} s^{-1} and 4.8×10^{-5} s^{-1} for CoA ester hydrolysis and MeSH release, respectively.

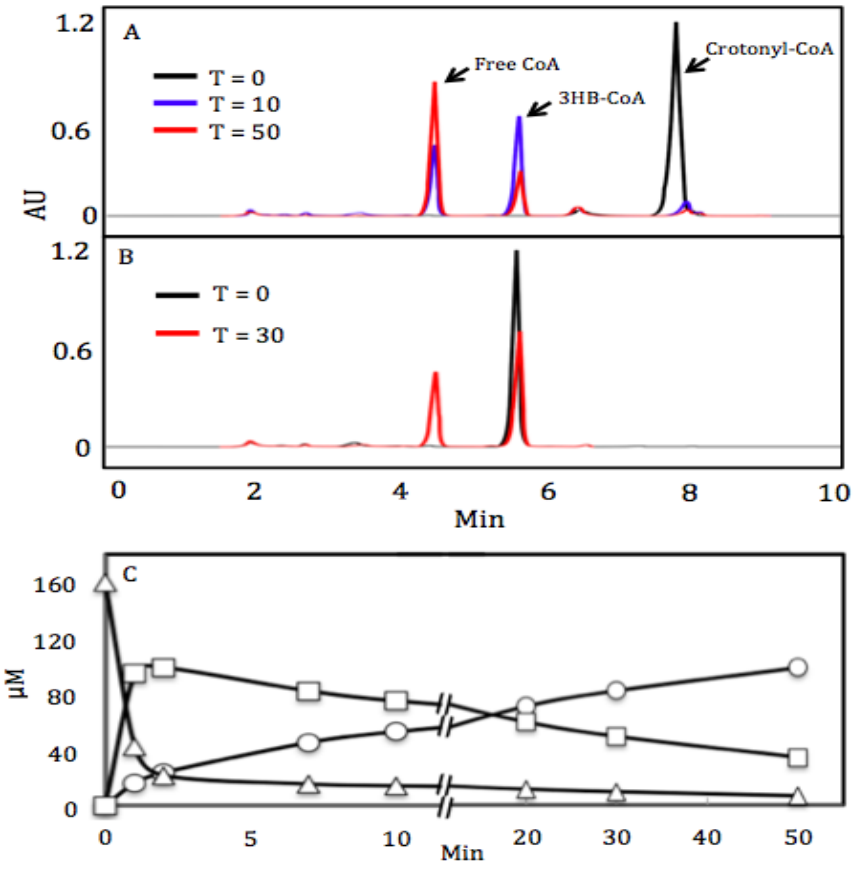

Figure 2.1. Reactions of DmdD with crotonyl-CoA and 3-hydroxybutyryl-CoA. Chromatography the DmdD reaction products following incubation with 160 μM crotonyl-CoA for 0, 10, and 50 min **(A)** or 3-hydroxybutyryl-CoA (3-HB-CoA) for 0 and 30 min **(B)**. AU is absorbance units. **(C)**. Reaction time course for the hydration/hydrolysis of crotonyl-CoA by DmdD. Crotonyl-CoA (Δ) is consumed at an initial rate of 90 μmol min^{-1} mg^{-1}. The formation of 3-hydroxybutyryl-CoA (□) and HS-CoA (○) occurs at initial rates of 72 μmol min^{-1} mg^{-1} and 12 μmol min^{-1} mg^{-1}, respectfully. After 2 min the rate of consumption of crotonyl-CoA proceeds at 0.94 μmol min^{-1} mg^{-1}. Consumption of 3-hydroxybutyryl-CoA occurs at 2.5 μmol min^{-1} mg^{-1}, while formation of free CoA proceeds at 3.3 μmol min^{-1} mg^{-1}.

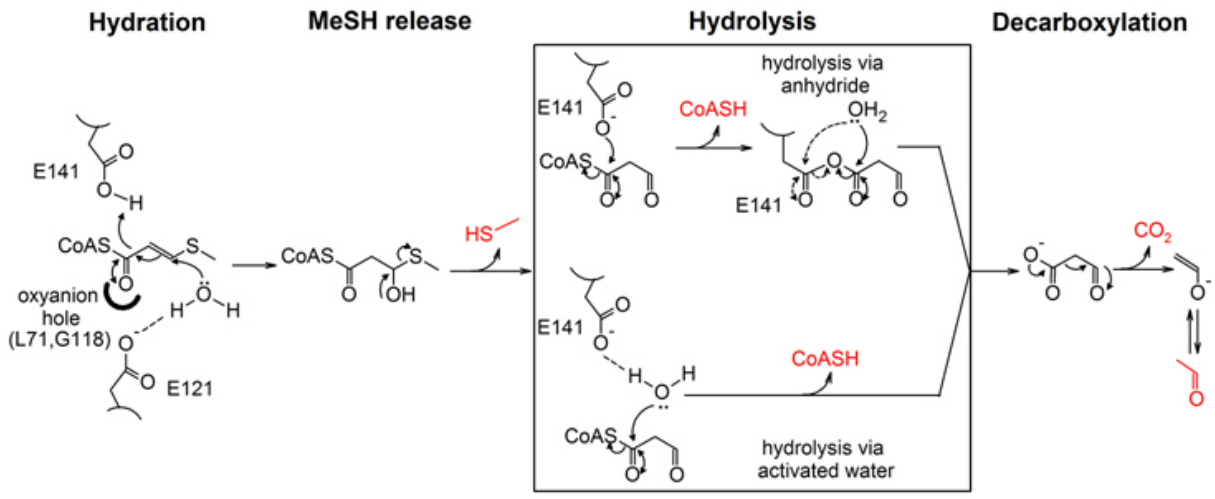

Figure 2.2. A proposed catalytic mechanism for the hydration and hydrolysis of MTA-CoA by DmdD. The products of the reaction are shown in red. For the hydrolysis of the anhydride in the anhydride mechanism, the hydroxyl group can attack either of the carbonyl carbons, as indicated by the two arrows.

Chapter 3

Assimilation of dimethylsulfoniopropionate carbon by *Ruegeria pomeroyi* DSS-3

3.1 Introduction

The marine phytoplankton metabolite dimethylsulfoniopropionate (DMSP) is ubiquitous in marine surface waters, making it one of the most abundant low molecular weight sources of carbon and reduced sulfur in the marine environment (7, 30, 33). Marine bacteria consume DMSP through two competing biochemical pathways, the demethylation pathway resulting in the release of methanethiol (MeSH) or the cleavage pathway producing dimethylsulfide (DMS). While some marine bacteria only possess one of these pathways (15), the model organism *Ruegeria pomeroyi* DSS-3 utilizes both. Recently, the biochemical pathway and genes responsible for the demethylation pathway were elucidated (35). This pathway starts with demethylation of DMSP by a tetrahydrofolate (THF)-dependent enzyme, DmdA, producing 5-methyl-THF and methylmercaptopropionate (MMPA). MMPA is then catabolized in a series of coenzyme-A mediated reactions analogous to fatty acid β-oxidation. The terminal step of the pathway results in the release of MeSH, CO_2, acetaldehyde, and free CoA. Acetaldehyde is further oxidized to acetate by an acetaldehyde dehydrogenase. Thus, the carbon from this pathway enters central carbon metabolism as acetate. *R. pomeroyi* is missing isocitrate lyase, the key enzyme in the glyoxylate shunt, but it does possess homologs for all the genes of the ethylmalonyl-CoA pathway (13). Therefore, *R. pomeroyi* was hypothesized to use the

ethylmalonyl-CoA pathway to assimilate the DMSP carbon that is routed through the demethylation pathway.

R. pomeroyi has four genes; *dddD, dddP, dddQ,* and *dddW,* that encode for proteins that catalyze the cleavage of DSMP, the initial step in the cleavage pathway. However, only mutations in *dddP, dddQ,* and *dddW* decreased DMSP cleavage by whole cells, while a mutation in *dddD* had no effect (44, 45). *dddP, dddQ,* and *dddW* all form acrylate in addition to DMS (27, 44, 45). However, the assimilation of acrylate in *R. pomeroyi* and other marine bacteria is poorly understood. Acrylate metabolism in a strain of *Halomonas* was extensively investigated by recombinant expression of several genes in *E. coli* (42). This work proposed a scheme in which acrylate is hydrated to 3-hydroxypropionate, which is further oxidized to malonate-semialdehyde. Malonate-semialdhyde is then decarboxylated, and acetyl-CoA is formed. Whether or not the first three steps are CoA- mediated reactions was not determined as these investigations were carried out in whole cells of *E. coli* and the enzymes were not purified.

Acryloyl-CoA is also part of the 3-hydroxypropionate pathway for CO_2 fixation described in the green nonsulfur phototrophic bacterium *Clhroroflexus auranticus* and the thermoacidophilic Archaea (1, 2). In this pathway, hydroxypropionate is converted to its CoA thioester, hydroxypropionyl-CoA, and then dehydrated to acryloyl-CoA before reduction to propionyl-CoA. In *C. auranticus,* these reactions are catalyzed by a trifunctional fusion protein. In contrast, members of the thermoacidophilic archaea *Sulfolobales* possess individual enzymes capable of catalyzing each of the three reactions.

Recently it was proposed that *Rhodobacter sphaeroides* assimilates 3-hydroxypropionate through a CoA-mediated pathway involving the dehydration of 3-hydroxypropionyl-CoA to acryloyl-CoA and then reduction to propionyl-CoA (38). The enzyme that catalyzes the

reduction of acryloyl-CoA in *R. pomeroyi* was recently identified by its ability to confer resistance to acrylate toxicity (43).

In this report the pathways used to assimilate DMSP in *R. pomeroyi* were investigated. DMSP carbon routed through the cleavage pathway was assimilated through acryloyl-CoA and propionyl-CoA (Figure 1). Two of the three enzymes that constitute this pathway were identified by purification from cell extracts and confirmed by recombinant expression. The fate of DMSP methyl groups was also investigated by using a ^{13}C tracer. This label was only incorporated into compounds biosynthesized via tetrahydrofolate-dependent pathways, indicating that cells do not have a robust C-1 metabolism when grown on DMSP.

3.2 Materials and Methods

Substrate synthesis

DMSP was synthesized as described previously (5) using 99% [1-^{13}C] acrylic acid (Sigma-Aldrich, St. Louis, MO) and dimethylsulfide or [$^{13}C_2$]dimethylsulfide (Cambridge Isotopes, Cambridge, MA) and acrylic acid. Acryloyl-CoA was synthesized with acryloyl-chloride and free coenzyme-A as described previously (28). The acryloyl-CoA was purified by reverse-phase chromatography using an Ultrasphere ODS preparative column (10 × 250 mm). The column was developed with 20 mM potassium phosphate (pH 6.8) and a gradient of 2–25% acetonitrile. Acryloyl-CoA was detected by its absorbance at 254 nm. Fractions containing acryloyl-CoA were lyophilized, resuspended in dH_2O, and again lyophilized. 3-Hydroxypropionyl-CoA was synthesized enzymatically from acryloyl-CoA with purified SPO0147 as described below. The product was purified by reverse phase chromatography as described above except that the buffer was 20 mM ammonium acetate, pH 6.0.

Growth of cultures

R. pomeroyi was grown at 30 °C in a carbon-limited chemostat with marine basal medium as described previously (34) using 2 mM DMSP at a flow rate of 0.1 ml min^{-1} and a dilution rate of 0.0416 h^{-1}. For labeling experiments, after five volumetric exchanges the outflow was collected into 100% ethanol, with the final concentration of ethanol being kept above 50%. Outflow was harvested daily by centrifugation at 10000 x g for 10 min, and the pellet was stored at -20 °C. For microarray experiments, cells were grown using the same conditions. Culture, 50 mL, was combined on ice with 5 mL of 95% ethanol/5% phenol and immediately centrifuged at 10000 x g for 5 min at -20 ^{o}C. The supernatant was decanted, and the cell pellet was stored at -80 ^{o}C until processing. For growth in batch cultures, *R. pomeroyi* wild-type and mutant strains were grown in batch culture using a marine basal medium as described previously (35). Cell material used for protein purifications was grown in a 1 L chemostat with a flow rate of 0.7 mL min^{-1} and a dilution rate of 0.042 hr^{-1} with 2 mM DMSP and 3 mM sodium acetate as the sources of carbon. After establishing steady state, approximately 900 mL of cell material was collected each day for three days. Collected cell material was harvested by centrifugation at 10000 x g for 10 min, washed with ice cold 50 mM Tris-HCl (pH 7.5), and then frozen at -20 ^{o}C. Cell material from three collections was resuspended in 2 mL buffer and lysed by bead beating for with 0.1 mm zirconia beads for 5 min using a vortex genie bead beating adapter (MoBio Laboratories). Cell lysate was centrifuged for 10 min at 10000 x g and then used for protein purifications. Calculations for the minimum enzymatic specific activity required to consume carbon entering the chemostat were performed as described previously (35), yielding a value of 57 nmol min^{-1} mg of $protein^{-1}$ for the conditions used in these experiments. Since 40% of DMSP is routed

through the cleavage pathway in the DMSP-limited chemostat (35), the minimum specific activity of enzymes in the cleavage pathway was 23 nmol min^{-1} mg of $protein^{-1}$.

Methanethiol and dimethylsulfide measurements

Methanethiol and dimethylsulfide were measured in the culture headspace by gas chromatography on an SRI 8610-C gas chromatograph with a Chromosil 330 column with nitrogen carrier gas at a flow rate of 60 ml min^{-1}, an oven temperature of 60 ^{o}C, and a flame photometric detector (8).

Enzyme Assays

Acrylate-CoA ligase was assayed in 50 mM HEPES (pH 7.5), 2 mM ATP, 2 mM $MgCl_2$, 0.05 mM CoA, and 2 mM acrylate. Reactions were initiated by the addition of cell extract. After 2-5 min, they were quenched by the addition of 4 µl H_3PO_4. After centrifugation to remove denatured proteins, the remaining CoA was analyzed by HPLC. Acryloyl-CoA hydratase activity was measured in 50 mM HEPES (pH 7.5) and 0.05 mM acryloyl-CoA. Reactions were initiated by the addition of protein and processed as described above. Activity was measured as the production of 3-hydroxypropionyl-CoA. Acryloyl-CoA reductase activity was measured in 50 mM HEPES (pH 7.5), 0.05 mM acryloyl-CoA or 3-hydroxypropionyl-CoA, 1 mM NADPH, and 1 mM $MgCl_2$. Reactions were initiated with the addition of protein. After 2-5 min, they were quenched and analyzed as described above. Activity was measured as the production of propionyl-CoA. Propionyl-CoA carboxylase activity was measured in 50 mM HEPES (pH 7.5), 0.05 mM propionyl-CoA, 2 mM ATP, 2 mM $MgCl_2$, and 10 mM $NaHCO_3$. Reactions were initiated with the addition of protein. After 2-5 min, they were quenched and analyzed. Activity

was measured by the disappearance of propionyl-CoA. Acetyl-CoA carboxylase activity was measured similarly except that acetyl-CoA was substituted for propionyl-CoA. Acetyl- and propionyl-CoA transferase activity was assayed in 50 mM HEPES (pH 7.5), 0.05 mM acetyl- or propionyl-CoA, and 2 mM sodium acrylate. Reactions were initiated by the addition of protein and quenched after 30 min. Activity was measured by the disappearance of either acetyl- or propionyl-CoA.

Genetic Modifications

Gene disruptions of SPO0370 and SPO1914 were made by homologous recombination of suicide plasmids as described previously (35). For the *pdh* mutant, random transposon mutagenesis was performed using an EZ-Tn5<KAN-2> Tnp Transposome kit (Epicentre), and the mutants were screened for their ability to reduce Ellman's reagent during growth with DMSP. One strain which grew poorly on DMSP, was identified, and the transposon insertion was mapped to position 83 of SPO2240 (*pdhA*) by Sanger sequencing at the Georgia Genomics Facility. For this reason, the strain was named pdh1.

Recombinant protein expression

Genes SPO1914, SPO0147, and SPO2934 were PCR amplified from *R. pomeroyi* genomic DNA and cloned into the pTrcHisA (Invitrogen) vector by standard techniques.

Protein purifications

For purification of the acryloyl-CoA hydratase (SPO0147) from *R. pomeroyi*, cell extract was applied to a Mono-Q HR anion exchange column (GE Healthcare, 1.6 x 10 cm) equilibrated with

50 mM Tris-HCl (pH 8.0) at a flow rate of 2 mL min^{-1}. Protein was eluted with a gradient from 0-1 M NaCl over 8 column volumes. Activity eluted between 18-28 mS/cm. Active fractions from the Mono-Q chromatography were pooled and made 1.7 M $(NH_4)_2SO_4$ by addition of solid $(NH_4)_2SO_4$. After centrifugation, the supernatant was applied to a phenyl-Superose HR hydrophobic interaction column (GE Healthcare, 1 x 10 cm) at a flow rate of 1 mL min^{-1}. The column was washed with one column volume of 1.7 M $(NH_4)_2SO_4$ in 50 mM Tris-HCl (pH 7.5). Protein was eluted with a gradient of 1.7-0 M $(NH_4)_2SO_4$ in 50 mM Tris-HCl (pH 7.5) over 7 column volumes. Activity eluted at 62-48 mS cm^{-1}. Active fractions were pooled and concentrated with an Amicon Ultra centrifugal filter (10 kD) to a final volume of about 0.2ml, then diluted to 5 mL with 5 mM potassium phosphate buffer (pH 7.5), and again concentrated to 0.2 mL. The final concentrate was then diluted to 1 ml in 5 mM potassium phosphate buffer (pH 7.5). The concentrated protein solution was then applied to a type-II hydroxyapatite column (1mL, BioRad) that was equilibrated with 5 mM potassium phosphate (pH 7.5) containing 1 mM $CaCl_2$. The column was washed with four column volumes of buffer, and protein was eluted with a 5-500 mM gradient of potassium phosphate buffer with 1 mM $CaCl_2$ over six column volumes. Activity eluted just after start of the gradient. The two 1 mL fractions containing the highest activity were concentrated using an Amicon Ultra centrifugal filter (10 kD). The acrylyl-CoA reductase (SPO1914) was purified as described above for the acryloyl-CoA hydratase. Activity co-eluted with acryloyl-CoA hydratase during anion-exchange chromatography. Activity eluted at 75-61 mS cm^{-1} after hydrophobic interaction chromatography. Active fractions were pooled, concentrated, and chromatographed with the hydroxyapatite column. Activity eluted after the start of the gradient. The two 1 mL fractions with the highest activity were concentrated as described above.

3.3 Results and Discussion

Acrylate-CoA ligase

Assuming that free acrylate was the product of DMSP cleavage by DddP, DddQ, or DddW (44), it was hypothesized that acryloyl-CoA was the next intermediate in the pathway of acrylate assimilation. To test this hypothesis, acrylate-CoA ligase activity was assayed in crude cell extracts of *R. pomeroyi* grown in a chemostat with DMSP as the sole source of carbon. Cell-free extracts provided with acrylate, HS-CoA, and ATP produced acryloyl-CoA at a rate of 24 nmol min^{-1} mg of $protein^{-1}$, which was sufficient to consume all of the substrate expected to pass through the cleavage pathway (see methods section for calculation). In contrast, acyl-CoA transferase activities from acetyl- or propionyl-CoA to acrylate were <1 nmol min^{-1} mg of $protein^{-1}$. Therefore, CoA ligase was the likely source of acryloyl-CoA.

It was hypothesized that the enzyme catalyzing the ligase reaction was encoded by the gene annotated as propionate-CoA ligase (*prpE,* EC# 6.2.1.17). This enzyme functions in the methylmalonyl-CoA pathway of propionate assimilation, and the enzymes from *Ralstonia solanacearum* and *Salmonella choleraesuis* possessed activity with both acrylate and propionate (32). To investigate the *prpE* from *R. pomeroyi,* the gene (SPO2934) was cloned and expressed in *E. coli*. Cell-free extracts of the recombinant *E. coli* had activity with both propionate and acrylate, while the host strain alone did not, supporting the hypothesis that the enzyme catalyzed both reactions in vivo. In addition, the microarray analysis showed that the *prpE* gene was up-regulated when grown on DMSP.

A mutant strain of *R. pomeroyi* was constructed in which a *tet* resistance cassette replaced most of the *prpE* gene. This mutant strain grew on propionate similarly to wild-type (Fig 2A).

This phenotype was also observed after mutation of the *prpE* gene in *Salmonella typhimurium*. In *S. typhimurium* a second mutation in the acetyl-CoA synthetase gene impaired the ability to grown on propionate, indicating that the acetyl-CoA synthetase was capable of complementing *prpE* (22). Likewise, *R. pomeroyi* has an acetyl-CoA synthetase as well as two forms of DmdB, which also possesses propionyl-CoA ligase activity (H. Bullock and C. Reisch, unpublished data). Thus, several enzymes may contribute to the ability of the *prpE* mutant to grow on propionate. The *R. pomeroyi prpE* mutant was also able to grow on acrylate and DMSP, although the growth rates were much decreased as compared to wild-type (Figure 2A). Again, the presence of several additional CoA-ligases may have contributed to the ability of this mutant to grow on acrylate. However, the diminished growth rate of the *prpE* mutant supports the hypothesis that acrylate-CoA ligases initiate the pathway of acrylate assimilation and are part of the DMSP-cleavage pathway.

Acryloyl-CoA hydratase

In cell-free extracts, acryloyl-CoA was rapidly converted to an unknown CoA-containing intermediate. To identify this compound, it was collected after HPLC separation and analyzed by Fourier Transformed Ion Cyclotron Resonance mass spectrometry (FTICR). The molecular mass was 839.14 Da, which was equal to the exact mass of acryloyl-CoA plus one water molecule. This datum suggested that acryloyl-CoA was hydrated to either 2- or 3-hydroxypropionyl-CoA. Since standards for these two compounds were neither commercially available nor easily synthesized, ^{1}H NMR was used to distinguish between them. Upon ^{1}H NMR analysis, the product of acryloyl-CoA hydration contained doublets at 2.6 and 3.8 ppm (data not shown), consistent with 3-hydroxypropionyl-CoA. If the product had been 2-hydroxypropionyl-

CoA, a distinctive doublet corresponding to the C-3 methyl group would have been located at 1.3 ppm. Thus, it was concluded that the product of acryloyl-CoA hydratase was 3-hydroxypropionyl-CoA. The specific activity of 3-hydroxypropionyl-CoA synthesis in cell extracts was >8 μmol min^{-1} mg of $protein^{-1}$, far exceeding the minimum activity required to support chemostat growth. This exceedingly high rate was consistent with the enzymatic efficiency of enoyl-CoA hydratases, which have been reported to be limited only by the rate of substrate diffusion (18).

The enzyme catalyzing the acryloyl-CoA hydration was identified by purification from cell extracts. A three-step purification, consisting of anion exchange, hydrophic interaction, and hydoxyapaptite chromatography, yielded a protein purified to electrophoretic homogeneity. The protein-encoding gene was identified by in-gel trypsin digestion and MALDI-TOF mass fingerprinting as SPO0147 and annotated as an enoyl-CoA hydratase. To confirm that this gene encoded for a protein with the correct catalytic function, the gene was cloned and expressed in *E. coli*. Cell extracts of the recombinant *E. coli* possessed acryloyl-CoA hydratase activity, while the host strain alone did not.

Acrolyl-CoA reductase

The fate of 3-hydroxypropionyl-CoA was next investigated in enzyme assays using cell-free extracts. In the absence of exogenous cofactors, cell free extracts did not consume 3-hydroxypropionyl-CoA. Upon the addition of NADH or NADPH, there was a quantitative conversion of 3-hydroxypropionyl-CoA to propionyl-CoA. This activity could be due to either an unprecedented 3-hydroxypropionyl-CoA reductase activity or coupling of the acryloyl-CoA hydratase with an acryloyl-CoA reductase activity (Figure 1). To clarify these results, the 3-

hydroxypropionyl-CoA reductase activity was partially purified from extracts of chemostat-grown cells. One of the three proteins remaining on a SDS-PAGE gel was identified by peptide mass fingerprinting as a zinc-dependent oxidoreductase encoded by gene SPO1914. To confirm the function of this gene product, SPO1914 was cloned and expressed in *E. coli*. The partially purified recombinant protein had activity for acryloyl-CoA reductase but not 3-hydroxypropionyl-CoA reductase. Thus, the 3-hydroxypropionyl-CoA reductase activity observed in cell extracts resulted from the coupling of the acryloyl-CoA hydratase with an acryloyl-CoA reductase activity.

To confirm the physiological significance of this activity, a mutant strain of *R. pomeroyi* was constructed in which SPO1914 was disrupted. The mutant was incapable of growth on acrylate or 3-hydroxypropionate (Figure 2B). In contrast, it grew similarly to wild-type when provided with propionate as the sole source of carbon. These results were consistent with the role of this enzyme in catalyzing the reduction of acryloyl-CoA to propionate during acrylate assimilation. The mutant strain also grew poorly on DMSP, with only 30% of inoculations capable of yielding growth similar to wild-type (data not shown). This result was unexpected as growth on DMSP should be possible since the demethylation pathway was uninterrupted. While the reason for this irregular growth phenotype was unclear, one possibility was that a build-up of acryloyl-CoA or 3-hydroxypropionyl-CoA in these cells caused a metabolic collapse due to shortage of free CoA. Lastly, the transcriptional response of gene SPO1914 was consistent with it being involved in DMSP metabolism, and in microarray experiments this gene was up-regulated 14-fold during growth on DMSP (Table 2).

Based in part upon its location, SPO1914 had previously been implicated in conferring acrylate resistance in *R. pomeroyi* as well as other proteobacteria (40). In *R. pomeroyi*, SPO1914

is adjacent to and predicted to be within the same transcriptional unit as *dmdA,* which encodes the enzyme that catalyzes the first step of the demethylation pathway. *Candidatus* Puniceispirillum marinum IMC1322, a member of the SAR116 clade of *Alphaproteobacteria*, also possessed an acryloyl-CoA reductase homolog with a protein identity of 62%. Interestingly, in this bacterium the gene was positioned immediately upstream of a *dddP* homolog, which encoded for a DMSP-cleavage enzyme (31), providing circumstantial evidence for a role in DMSP metabolism in this bacterium as well. Similarly, the *R. sphaeroides* homolog, called *acuI* for acrylate incorporation, was coexpressed with the *dddL* gene during growth on DMSP (39). Although this bacterium does not grow on acrylate, this gene was implicated in increased resistance to acrylate toxicity and acrylate degradation by resting cells.

Assimilation of the propionyl carbons from DMSP

Only a small portion of the label from [1-^{13}C] DMSP was assimilated during chemostat growth. During growth with 99% enriched [1-^{13}C] DMSP, the $^{13}C/^{12}C$ of the cells and carbonate (sum of CO_2 + HCO_3^- + H_2CO^3) produced were 9.2% and 28%, respectively. Based upon total cellular and carbonate production rates of 300 and 540 nmol C min^{-1}, respectively, the ^{13}C-cellular and ^{13}C-carbonate production rates were 28 and 171 nmol min^{-1} (Table 3). The sum of these values, 199 nmol min^{-1}, was close to the expected value of 206 nmol min^{-1}, verifying the nearly complete metabolism of DMSP and the accuracy of the measurements. The small amount of label appearing in cells suggested that most of the C-1 carbon of DMSP was oxidized to CO_2.

Based upon the expected fluxes through the demethylation and cleavage pathways, the fluxes of individual intermediates were solved algebraically to yield the estimated levels of CO_2 from respiration and intermediates needed for growth. During growth in the chemostat, the flux

through the cleavage pathway was equal to the amount of DMS produced or 80 nmol min^{-1} and yielded acryloyl-CoA. The remaining 120 nmol min^{-1} was routed through the demethylation pathway and produced acetaldehyde, which would be metabolized to acetate and acetyl-CoA. Acetyl-CoA was assumed to be assimilated by the ethylmalonyl-CoA pathway. The fluxes of intermediates necessary to support growth of 300 nmol min^{-1} cellular C were 21 nmol min^{-1} of acetyl-CoA, 20 nmol min^{-1} of pyruvate, 50 nmol min^{-1} of oxaloacetate, and 7 nmol min^{-1} of α-ketogluturate. Given these constraints, it was not possible to solve pathways that did not include a significant flux through the pyruvate dehydrogenase complex (Fig. 3). Moreover, pathways could not be solved that included a significant role for malate and α-ketogluturate oxidation via the TCA cycle or the serine cycle enzymes for the transformation of glyoxylate to either phosphoenolpyruvate for carbon assimilation or malyl-CoA for oxidation in the TCA cycle.

Based upon this predicted pathway, the ^{13}C-labeling of whole cells was expected to be 8.8% or close to the measured value of 9.2%. The labeling of the internal carbonate pool was assumed not to be in equilibrium with the external carbonate pool. For the labeling of the internal pool, 195 nmol min^{-1} of C-1 DMSP carbons were estimated to be oxidized to carbonate, and the total carbonate production from DMSP was estimated to be 592 nmol min^{-1}. After accounting for the natural abundance, the internal pool carbonate pool was estimated to be enriched by 34%. Given the dilution of the net cellular production of carbonate of 540 nmol min^{-1} by 70 nmol min^{-1} carbonate from aeration, the enrichment of the external carbonate pool was estimated to be 30% or close to the observed value of 28%. These comparisons between the estimated and observed enrichments for cells and carbonate provided a further test for the proposed pathway.

The labeling patterns of key amino acids from [1-^{13}C] DMSP supported for this pathway of carbon assimilation. The C-1 and C-4 carbons of aspartate were enriched by 40% and 32%,

respectively (Table 4). This pattern was consistent with the formation of aspartate from malate via oxaloacetate and two sources of malate in the DMSP-grown cells (Fig. 3). Part of the malate would be formed from succinyl-CoA via succinate. Because succinate is symmetrical, the enrichment of the C-1 and C-4 carbons formed via this route would be identical. The remaining malate would be formed from malyl-CoA via the ethylmalonyl-CoA pathway. For this malate, the C-1 would be enriched due to the incorporation of enriched CO_2, but the C-4 would not be enriched. For the fluxes calculated in Figure 4, the theoretical enrichments for the C-1 and C-4 carbons of aspartate were 37% and 26%, respectively, or close to the observed enrichments. Similarly, the theoretical enrichment for the C-1 of pyruvate, 37%, was close to the observed value of 39%.

The labeling patterns of leucine and valine were consistent with their formation from pyruvate and acetyl-CoA as predicted by the canonical pathway for branched-chain amino acid biosynthesis (data not shown). However, isoleucine possessed no highly enriched carbons, which indicated that it was not derived from threonine (data not shown). This observation was consistent with the alternative pathway for isoleucine synthesis in which acetyl-CoA and pyruvate form citramalate (11, 36). Isoleucine synthesized by this pathway would not contain any highly enriched carbons.

Phenotype of a pyruvate dehydrogenase mutant

To verify the role of the pyruvate dehydrogenase complex in DMSP metabolism, a mutant with a transposon insertion in the gene encoding the α-subunit of pyruvate dehydrogenase was characterized. The mutant grew poorly on DMSP, supporting the proposed role of pyruvate dehydrogenase in DMSP metabolism (Fig. 4). Growth on MMPA and acetate was

indistinguishable from wild type, suggesting that cells were able to overcome the mutation during growth on these substrates. In contrast, the mutant was unable to grow with propionate as the sole carbon source. When both propionate and acetate were present, the mutant exhibited growth identical to the wild-type (Fig. 4). Similarly, the mutant grew poorly on succinate, and growth was restored to wild-type levels by acetate (data not shown). Carbonate had no effect on growth of the mutant on propionate, indicating that poor growth was not due to CO_2 limitation for succinate biosynthesis. These results suggested that pyruvate dehydrogenase played an important oxidative role during growth on electron-rich substrates such as propionate, succinate and DMSP (Fig. 3).

Discussion

Acrylate assimilation

R. pomeroyi possesses two routes of DMSP catabolism. The first route, known as the demethylation pathway, is initiated by the enzyme DmdA, which transfers a methyl group from DMSP to THF, producing 5-methyl-THF and methylmercaptopropionate (MMPA). MMPA is then catabolized in a series of coenzyme-A- mediated reactions, releasing MeSH, CO_2, and acetate (35, 42). The second route is the DMSP cleavage pathway and results in the production of DMS and a three carbon moiety identified as acrylate or 3-hydroxypropionate. Four gene products in *R. pomeroyi* catalyze the cleavage reaction for DMS formation (41, 44, 46). Mutations in three of these genes, *dddP, dddQ,* and *dddW* affected DMS production during growth on DMSP and were functional under the conditions tested. In contrast, a mutation in the fourth gene, *dddD*, had no effect, and its physiological importance is not clear. Upon purification, DddP was shown to produce acrylate in addition to DMS. Cell free extracts of *E.*

coli expressing DddW also formed acrylate, but the enzyme has not been purified *in R. pomeroyi*. Likewise, DddQ has not been characterized *in-vitro*, but in whole cells experiments *E. coli* expressing DddQ produced acrylate in the presence of DMSP, suggesting that acrylate was in fact the product of DddQ. The purpose of the investigations here was to establish the pathway for DMSP and acrylate assimilation in *R. pomeroyi*.

The genome of *R. pomeroyi* encodes three enzymes which carboxylate C3 substrates to form a C4 moiety that could enter the TCA cycle and possibly be involved in metabolism of the C-3 moiety formed in DMSP cleavage: pyruvate carboxylase, phosphoenolpyruvate carboxylase, and propionyl-CoA carboxylase, (29). Of these genes, only propionyl-CoA carboxylase was up-regulated in the microarray experiments during growth on DMSP. Furthermore, the other enzymes in the methylmalonyl-CoA pathway for C3 assimilation were up-regulated during growth on DMSP. These microarray results were consistent with previous experiments which found that DMSP caused a significant up-regulation of propionate assimilation genes (3, 48). Thus, these results are consistent with the role of the methylmalonyl-CoA pathway in DMSP assimilation.

Transcriptional response studies and bioinformatics analysis are complicated by the fact that a number of metabolic pathways share common intermediates and enzymes. For example, the ethylmalonyl-CoA pathway for C2 assimilation includes components of the methylmalonyl-CoA pathway for propionyl-CoA assimilation. Thus, observations of increased expression of C3 metabolic genes may be a physiological response to C2 compounds. Given the recent identification of the MMPA-CoA pathway, which results in acetate production, up-regulation of propionate assimilation genes is expected regardless of whether the DMSP demethylation or cleavage pathway is being utilized. However, the propionate-CoA ligase gene, which is

proposed to physiologically function as an acrylate-CoA ligase as well, is not part of the ethylmalonyl-CoA pathway. Thus, the up-regulation of this gene during growth with DMSP is strong evidence for its participation in acrylate assimilation.

To determine the pathway for assimilation of carbon routed through the cleavage pathway, enzyme assays were used to reconstruct the metabolic pathway. Enzyme assays revealed that cell extracts were capable of catalyzing the production of acryloyl-CoA, which is then reduced to propionyl-CoA. In a side reaction, acryloyl-CoA is rapidly hydrated to 3-hydroxypropionyl-CoA. This side reaction may be a mechanism for protecting the cell against the toxic effects of acryloyl-CoA.

The recently described ethylmalonyl-CoA pathway is used for acetate assimilation in many isocitrate lyase-negative bacteria. The diagnostic gene in this pathway, *ccr*, encodes for the crotonyl-CoA carboxylase/reductase, which carboxylates crotonyl-CoA to ethymalonyl-CoA (12). In the isocitrate lyase negative bacteria *Methylobacter extorquens* and *Streptomyces coelicor,* a mutation in *ccr* yielded strains incapable of growth on acetate (6, 19). Accordingly, a strain of *R. pomeroyi* with a disruption of the *ccr* gene was also incapable of growth on acetate and had a serious defect with growth on MMPA. These results confirm that the ethylmalonyl-CoA pathway is used for acetate assimilation in *R. pomeroyi* and support the hypothesis that MMPA is assimilated as acetate. While the mutant strain was able to grow on MMPA after an extended lag phase, the growth yield was greatly reduced compared to wild-type. The reason for this leaky phenotype is currently under investigation.

Methyl carbon assimilation

R. pomeroyi grown in a chemostat with [^{13}C-methyl] DMSP resulted in cell material with only a few carbons highly enriched in ^{13}C. Each of these enrichments can be attributed to methyl group donations from THF single carbon carriers. Serine was enriched by 30% in the C-3 position. This labeling was consistent with the transfer of an enriched methylene group from methylene-THF to glycine, in a reaction catalyzed by serine hydroxymethyltransferase. The remaining 70% of serine is probably biosynthesized via 3-phosphoglycerate derived from gluconeogenesis. Not unexpectedly, the serine hydroxymethyltransferase gene was significantly up-regulated in microarray experiments.

There were two possible sources for the enriched C1 unit that appeared in serine. First, 5-methyl-THF produced by DmdA during the initial demethylation of DMSP may be oxidized to 5-methylene-THF, which may then be directly utilized by serine hydroxymethyltransferase. The genome sequence of *R. pomeroyi* contains a *metF* homolog, which reduces methylene-THF to 5-methyl-THF. This reaction is reversible, so it is possible that the physiological reaction under these conditions was to oxidize 5-methyl-THF. Alternatively, the methyl group of methanethiol may be oxidized to formaldehyde, which spontaneously reacts with THF to form methylene-THF. Several enzymes that catalyze the oxidation of methanethiol to formaldehyde, hydrogen sulfide, and hydrogen peroxide have been purified and characterized (16, 26, 40). However, the genes encoding these enzymes have not been identified, and this activity has not yet been examined in *R. pomeroyi*.

The methyl group of methionine was enriched to 99% ^{13}C under these conditions. There are two possible explanations for this high enrichment. Previous experiments have shown that ^{35}S sulfur from DMSP is assimilated into the cellular amino acids of marine bacteria (25). It was

hypothesized that a direct incorporation of methanethiol into homoserine was catalyzed by cystathionine γ-synthase and may be responsible for this production of methionine (23). However, the gene for this enzyme is absence from *R. pomeroyi*, so there may be an alternative source of this activity. *R. pomeroyi* possesses the gene for methionine γ-lyase, which catalyzes the release of methanethiol from methionine. Growth of *R. pomeroyi* on methionine also results in the production of methanethiol (C.R. Reisch unpublished observation), indicating that this activity is present in whole cells under these conditions. It is possible that this enzyme works in the reverse direction to catalyze the direct incorporation of methanethiol. The second possible source of highly enriched methyl groups is from 5-methyl-THF. The last step of the canonical pathway of methionine biosynthesis transfers a methyl group from 5-methyl-THF to homocysteine. Since the initial demethylation of DMSP produces 5-methyl-THF, there should be an abundance of highly enriched 5-methyl-THF available for methionine biosynthesis.

The biosynthesis of purine nucleosides is the third reaction for which a THF derivative provides a single carbon unit. Of the five carbons present in the purines, only the carbon derived from formyl-THF is highly enriched. Formyl-THF may be derived from two different sources. First, 10-methylene-THF is oxidized to 5-10-methenyl-THF and subsequently hydrated to formyl-THF. Two enzymes, MtdA or MtdB, that catalyze the first reaction have been identified in some *Alphaproteobacteria*, although not in *R. pomeroyi* (17, 49). *R. pomeroyi* does have two FolD homologs, which are annotated as methylenetetrahydrofolate dehydrogenase/methenyltetrahydrofolate cyclohydrase (DHCH) proteins. Functional DHCH proteins oxidize 5-10-methylene-THF to 5-10-methenyl-THF and hydrolyze the latter to form 10-formyl-THF (9). Second, formyl-THF may be synthesized by formate-THF ligase. This ATP-dependent enzyme forms 10-formyl-THF from free formate and THF. The genome

sequence of *R. pomeroyi* contains two formate-THF ligase homologs with identical protein sequences. The 90% enrichment in carbons derived from formyl-THF suggests that both pathways of formyl-THF synthesis may be active. If all of the formyl-THF was derived directly from methylene-THF, an enrichment of 99% would be expected, consistent with the enrichment of methionine. However, the data suggests that there is a source of formate that is not derived from the methyl groups of DMSP and would therefore dilute the enriched pool to 90%. *R. pomeroyi* possesses several genes annotated as formate dehydrogenases which could provide this unenriched carbon.

3.5 References

1. **Alber, B. E., and G. Fuchs.** 2002. Propionyl-coenzyme A synthase from *Chloroflexus aurantiacus*, a key enzyme of the 3-hydroxypropionate cycle for autotrophic CO_2 fixation. J Biol Chem **277:**12137-12143.
2. **Berg, I. A., D. Kockelkorn, W. Buckel, and G. Fuchs.** 2007. A 3-hydroxypropionate/4-hydroxybutyrate autotrophic carbon dioxide assimilation pathway in archaea. Science **318:**1782-1786.
3. **Burgmann, H., E. C. Howard, W. Ye, F. Sun, S. Sun, S. Napierala, and M. A. Moran.** 2007. Transcriptional response of Silicibacter pomeroyi DSS-3 to dimethylsulfoniopropionate (DMSP). Environ Microbiol **9:**2742-2755.
4. **Carter, H. E., and C. M. Stevens.** 1941. Benzyoylation of amino acids. J Biol Chem **138:**627-629.
5. **Chambers, S. T., C. M. Kunin, D. Miller, and A. Hamada.** 1987. Dimethylthetin can substitute for glycine betaine as an osmoprotectant molecule for *Escherichia coli*. J Bacteriol **169:**4845-4847.
6. **Chistoserdova, L. V., and M. E. Lidstrom.** 1996. Molecular characterization of a chromosomal region involved in the oxidation of acetyl-CoA to glyoxylate in the isocitrate-lyase-negative methylotroph *Methylobacterium extorquens* AM1. Microbiol-Uk **142:**1459-1468.
7. **Curson, A. R., J. D. Todd, M. J. Sullivan, and A. W. Johnston.** 2011. Catabolism of

dimethylsulphoniopropionate: microorganisms, enzymes and genes. Nature Rev Microbiol **9:**849-859.

8. **de Souza, M. P., and D. C. Yoch.** 1995. Purification and characterization of dimethylsulfoniopropionate lyase from an Alcaligenes-like dimethyl sulfide-producing marine isolate. Appl Environ Microbiol **61:**21-26.

9. **Dev, I. K., and R. J. Harvey.** 1978. A complex of N5,N10-methylenetetrahydrofolate dehydrogenase and N5,N10-methenyltetrahydrofolate cyclohydrolase in *Escherichia coli*. Purification, subunit structure, and allosteric inhibition by N10-formyltetrahydrofolate. J Biol Chem **253:**4245-4253.

10. **Eisenreich, W., G. Strauss, U. Werz, G. Fuchs, and A. Bacher.** 1993. Retrobiosynthetic analysis of carbon fixation in the phototrophic eubacterium *Chloroflexus aurantiacus*. Eur J Biochem **215:**619-632.

11. **Ekiel, I., I. C. Smith, and G. D. Sprott.** 1983. Biosynthetic pathways in *Methanospirillum hungatei* as determined by ^{13}C nuclear magnetic resonance. J Bacteriol **156:**316-326.

12. **Erb, T. J., I. A. Berg, V. Brecht, M. Muller, G. Fuchs, and B. E. Alber.** 2007. Synthesis Of C-5-dicarboxylic acids from C-2-units involving crotonyl-CoA carboxylase/reductase: The ethylmalonyl-CoA pathway. P Natl Acad Sci USA **104:**10631-10636.

13. **Erb, T. J., G. Fuchs, and B. E. Alber.** 2009. (2S)-Methylsuccinyl-CoA dehydrogenase closes the ethylmalonyl-CoA pathway for acetyl-CoA assimilation. Mol Microbiol **73:**992-1008.

14. **Friedrich, C. G., D. Rother, F. Bardischewsky, A. Quentmeier, and J. Fischer.** 2001.

Oxidation of reduced inorganic sulfur compounds by bacteria: Emergence of a common mechanism? Appl Environ Microbiol **67:**2873-2882.

15. **Gonzalez, J. M., R. P. Kiene, and M. A. Moran.** 1999. Transformation of sulfur compounds by an abundant lineage of marine bacteria in the alpha-subclass of the class Proteobacteria. Appl Environ Microbiol **65:**3810-3819.

16. **Gould, W. D., and T. Kanagawa.** 1992. Purification and properties of methyl mercaptan oxidase from *Thiobacillus thioparus* TK-m. J Gen Microbiol **138:**217-221.

17. **Hagemeier, C. H., L. Chistoserdova, M. E. Lidstrom, R. K. Thauer, and J. A. Vorholt.** 2000. Characterization of a second methylene tetrahydromethanopterin dehydrogenase from *Methylobacterium extorquens* AM1. Eur J Biochem **267:**3762-3769.

18. **Hamed, R. B., E. T. Batchelar, I. J. Clifton, and C. J. Schofield.** 2008. Mechanisms and structures of crotonase superfamily enzymes - How nature controls enolate and oxyanion reactivity. Cell Mol Life Sci **65:**2507-2527.

19. **Han, L., and K. A. Reynolds.** 1997. A novel alternate anaplerotic pathway to the glyoxylate cycle in streptomycetes. J Bacteriol **179:**5157-5164.

20. **Henriksen, J. R.** 2008. Physiology of dimethylsulfoniopropionate metabolism in a model marine Roseobacter, *Silicibacter pomeroyi.* University of Georgia, Athens.

21. **Hetzel, M., M. Brock, T. Selmer, A. J. Pierik, B. T. Golding, and W. Buckel.** 2003. Acryloyl-CoA reductase from *Clostridium propionicum*. An enzyme complex of propionyl-CoA dehydrogenase and electron-transferring flavoprotein. Eur J Biochem **270:**902-910.

22. **Horswill, A. R., and J. C. Escalante-Semerena.** 1999. The *prpE* gene of *Salmonella typhimurium* LT2 encodes propionyl-CoA synthetase. Microbiol-Uk **145:**1381-1388.

23. **Kanzaki, H., M. Kobayashi, T. Nagasawa, and H. Yamada.** 1987. Purification and characterization of cystathionine gamma-synthase type-II from *Bacillus sphaericus*. Eur J Biochem **163:**105-112.

24. **Kiene, R. P., L. J. Linn, and J. A. Bruton.** 2000. New and important roles for DMSP in marine microbial communities. J. Sea. Res **43:**209-224.

25. **Kiene, R. P., L. J. Linn, J. Gonzalez, M. A. Moran, and J. A. Bruton.** 1999. Dimethylsulfoniopropionate and methanethiol are important precursors of methionine and protein-sulfur in marine bacterioplankton. Appl Environ Microbiol **65:**4549-4558.

26. **Kim, S. J., H. J. Shin, Y. C. Kim, D. S. Lee, and J. W. Yang.** 2000. Isolation and purification of methyl mercaptan oxidase from *Rhodococcus rhodochrous* for mercaptan detection. Biotechnol Bioloproc E **5:**465-468.

27. **Kirkwood, M., N. E. Le Brun, J. D. Todd, and A. W. B. Johnston.** 2010. The dddP gene of *Roseovarius nubinhibens* encodes a novel lyase that cleaves dimethylsulfoniopropionate into acrylate plus dimethyl sulfide. Microbiol-SGM **156:**1900-1906.

28. **Kuchta, R. D., and R. H. Abeles.** 1985. Lactate reduction in *Clostridium propionicum* - purification and properties of lactyl-Coa dehydratase. J. Biol. Chem. **260:**3181-3189.

29. **Moran, M. A., A. Buchan, J. M. Gonzalez, J. F. Heidelberg, W. B. Whitman, R. P. Kiene, J. R. Henriksen, G. M. King, R. Belas, C. Fuqua, L. Brinkac, M. Lewis, S. Johri, B. Weaver, G. Pai, J. A. Eisen, E. Rahe, W. M. Sheldon, W. Ye, T. R. Miller, J. Carlton, D. A. Rasko, I. T. Paulsen, Q. Ren, S. C. Daugherty, R. T. Deboy, R. J. Dodson, A. S. Durkin, R. Madupu, W. C. Nelson, S. A. Sullivan, M. J. Rosovitz, D. H. Haft, J. Selengut, and N. Ward.** 2004. Genome sequence of Silicibacter pomeroyi

reveals adaptations to the marine environment. Nature **432:**910-913.

30. **Moran, M. A., C. R. Reisch, R. P. Kiene, and W. B. Whitman.** 2012. Genomic insights into bacterial DMSP transformations. Annu Rev Mar Sci **4:**523-542.

31. **Oh, H. M., K. K. Kwon, I. Kang, S. G. Kang, J. H. Lee, S. J. Kim, and J. C. Cho.** 2010. Complete genome sequence of "Candidatus Puniceispirillum marinum" IMCC1322, a representative of the SAR116 clade in the Alphaproteobacteria. J Bacteriol **192:**3240-3241.

32. **Rajashekhara, E., and K. Watanabe.** 2004. Propionyl-coenzyme A synthetases of *Ralstonia solanacearum* and *Salmonella choleraesuis* display atypical kinetics. FEBS Lett **556:**143-147.

33. **Reisch, C. R., M. A. Moran, and W. B. Whitman.** 2011. Bacterial catabolism of dimethylsulfoniopropionate (DMSP). Frontiers Microbiol **2:**172.

34. **Reisch, C. R., M. A. Moran, and W. B. Whitman.** 2008. Dimethylsulfoniopropionate-dependent demethylase (DmdA) from *Pelagibacter ubique* and *Silicibacter pomeroyi*. J Bacteriol **190:**8018-8024.

35. **Reisch, C. R., M. J. Stoudemayer, V. A. Varaljay, I. J. Amster, M. A. Moran, and W. B. Whitman.** 2011. Novel pathway for assimilation of dimethylsulphoniopropionate widespread in marine bacteria. Nature **473:**208-211.

36. **Risso, C., S. J. Van Dien, A. Orloff, D. R. Lovley, and M. V. Coppi.** 2008. Elucidation of an alternate isoleucine biosynthesis pathway in Geobacter sulfurreducens. J Bacteriol **190:**2266-2274.

37. **Roberts, R. B.** 1955. Studies of biosynthesis in *Escherichia coli*. Carnegie Institution of Washington, Washington,.

38. **Schneider, K., M. Asao, M. S. Carter, and B. E. Alber.** 2012. *Rhodobacter sphaeroides* uses a reductive route via propionyl coenzyme A to assimilate 3-hydroxypropionate. J Bacteriol **194:**225-232.

39. **Sullivan, M. J., A. R. Curson, N. Shearer, J. D. Todd, R. T. Green, and A. W. Johnston.** 2011. Unusual regulation of a leaderless operon involved in the catabolism of dimethylsulfoniopropionate in *Rhodobacter sphaeroides*. PLoS One **6:**e15972.

40. **Suylen, G. M. H., P. J. Large, J. P. Van Dijken, and J. G. Kuenen.** 1987. Methyl mercaptan oxidase, a key enzyme in the metabolism of methylated sulphur compounds by *Hyphomicrobium* EG. J Gen Microbiol **133:**2989-2997.

41. **Todd, J. D., A. R. Curson, C. L. Dupont, P. Nicholson, and A. W. Johnston.** 2009. The *dddP* gene, encoding a novel enzyme that converts dimethylsulfoniopropionate into dimethyl sulfide, is widespread in ocean metagenomes and marine bacteria and also occurs in some Ascomycete fungi. Environ Microbiol **11:**1376-1385.

42. **Todd, J. D., A. R. Curson, N. Nikolaidou-Katsaraidou, C. A. Brearley, N. J. Watmough, Y. Chan, P. C. Page, L. Sun, and A. W. Johnston.** 2009. Molecular dissection of bacterial acrylate catabolism - unexpected links with dimethylsulfoniopropionate catabolism and dimethyl sulfide production. Environ Microbiol.

43. **Todd, J. D., A. R. Curson, M. J. Sullivan, M. Kirkwood, and A. W. Johnston.** 2012. The Ruegeria pomeroyi acuI gene has a role in DMSP catabolism and resembles yhdH of E. coli and other bacteria in conferring resistance to acrylate. PloS one **7:**e35947.

44. **Todd, J. D., A. R. J. Curson, M. Kirkwood, M. J. Sullivan, R. T. Green, and A. W. B. Johnston.** 2011. DddQ, a novel, cupin-containing, dimethylsulfoniopropionate lyase

in marine roseobacters and in uncultured marine bacteria. Environ Microbiol **13:**427-438.

45. **Todd, J. D., M. Kirkwood, S. Newton-Payne, and A. W. Johnston.** 2011. DddW, a third DMSP lyase in a model Roseobacter marine bacterium, *Ruegeria pomeroyi* DSS-3. ISME J.

46. **Todd, J. D., R. Rogers, Y. G. Li, M. Wexler, P. L. Bond, L. Sun, A. R. Curson, G. Malin, M. Steinke, and A. W. Johnston.** 2007. Structural and regulatory genes required to make the gas dimethyl sulfide in bacteria. Science **315:**666-669.

47. **Tusher, V. G., R. Tibshirani, and G. Chu.** 2001. Significance analysis of microarrays applied to the ionizing radiation response. P Natl Acad Sci USA **98:**5116-5121.

48. **Vila-Costa, M., J. M. Rinta-Kanto, S. Sun, S. Sharma, R. Poretsky, and M. A. Moran.** 2010. Transcriptomic analysis of a marine bacterial community enriched with dimethylsulfoniopropionate. ISME J **4:**1410-1420.

49. **Vorholt, J. A., L. Chistoserdova, M. E. Lidstrom, and R. K. Thauer.** 1998. The NADP-dependent methylene tetrahydromethanopterin dehydrogenase in *Methylobacterium extorquens* AM1. J Bacteriol **180:**5351-5356.

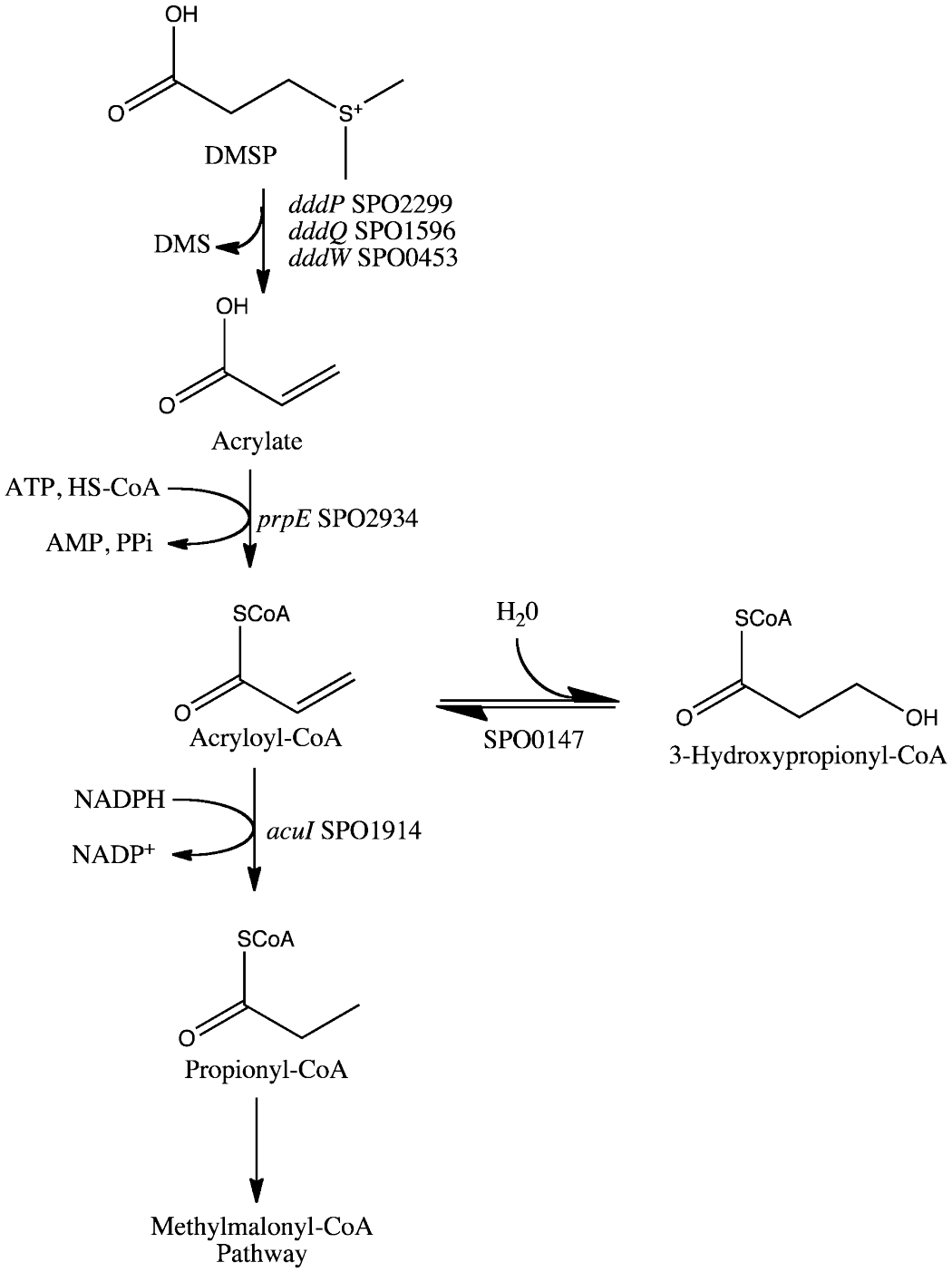

Figure 3.1. Proposed DMSP cleavage and acrylate assimilation pathway in *R. pomeroyi*.

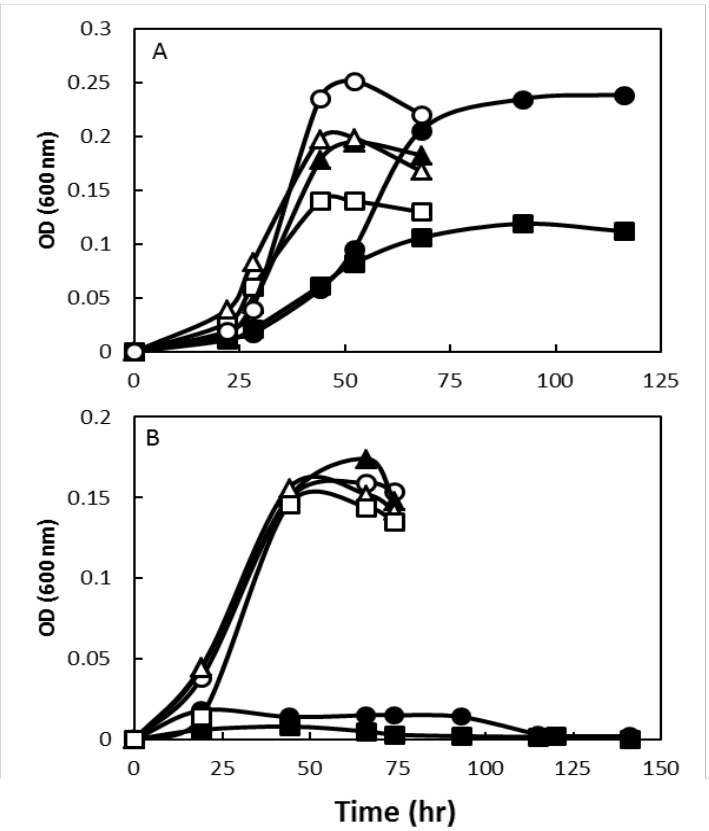

Figure 3.2. Growth of wild-type *R. pomeroyi* and mutant strains. (**A)** Growth of wild-type *R. pomeroyi* and the *prpE* mutant SPO2934::*tet*. Wild-type cells grown with 3 mM acrylate (□), DMSP (○), and propionate (Δ). SPO2934::*tet* grown with 3 mM acrylate (■), DMSP (●), and propionate (▲). (B) Growth of wild-type *R. pomeroyi* and the *acuI* mutant SPO1914::*tet*. Wild-type cells grown with 3 mM propionate (Δ), acrylate (□), and 3-hydroxypropionate (○). SPO1914::*tet* grown with 3 mM propionate (▲), acrylate (■), 3-hydroxypropionate (●).

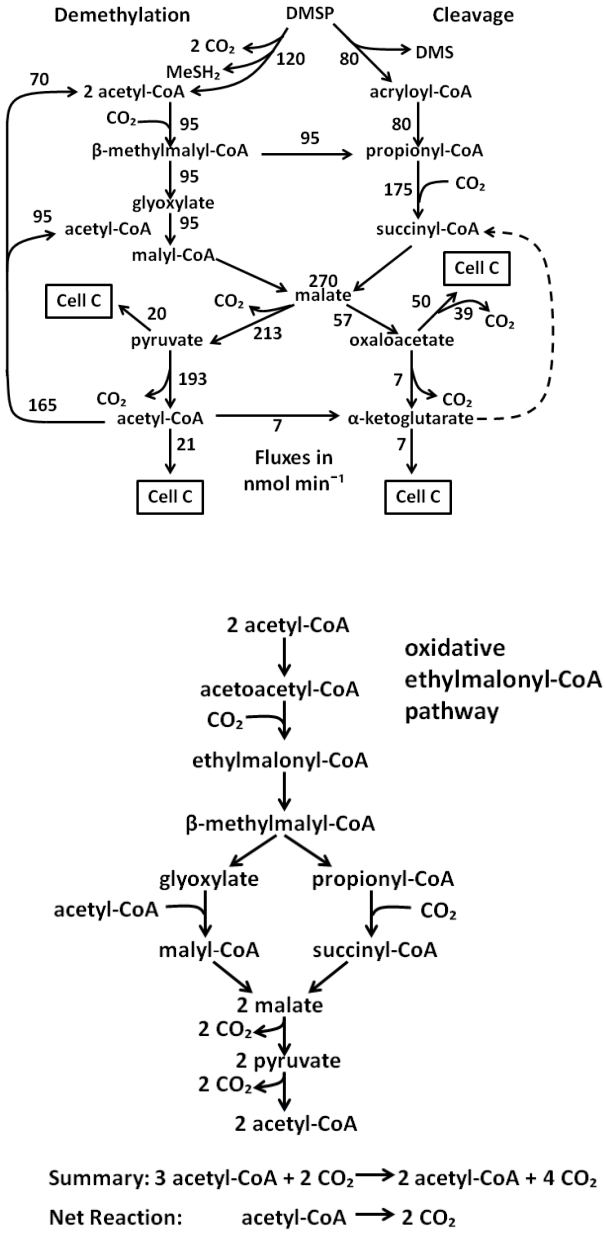

Figure 3.3. **(A).** Carbon fluxes during DMSP assimilation and oxidation. Only key intermediates of the demethylation and cleavage pathways are shown. **(B.)** Oxidative ethylmalonyl-CoA pathway for growth on electron-rich substrates.

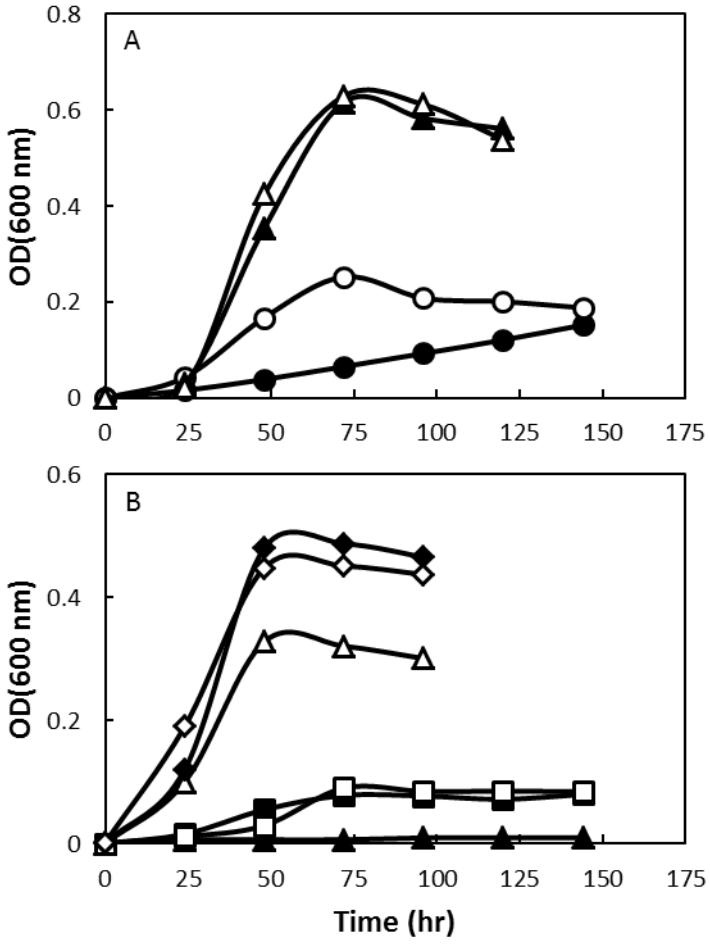

Figure 3.4. Growth phenotype of wild-type *R. pomeroyi* and the *pdhA::Tn5* mutant pdh1. (**A**) Growth of the wild-type cells with 5 mM MMPA (Δ) and 3 mM DMSP (○) and pdh1 mutant with 5 mM MMPA (▲) and 3 mM DMSP (●). (**B**) Growth of the wild-type cells with 3 mM acetate (□), propionate (Δ), and 3 mM acetate + 3 mM propionate (◊) and the pdh1 mutant with 3 mM acetate (■) propionate (▲) and 3 mM acetate + 3 mM propionate (◆)

Chapter 4

Metabolism of One-Carbon Compounds

4.1 Introduction

C-1 compounds, such as methanol, formaldehyde, formate and methylamine, play a central role in microbial metabolism. Methylotrophs, the best studies of these organisms, oxidize methyl groups and C-1 compounds to derive energy and cellular carbon via the ribulose monophosphate (RuMP) or serine cycle pathways (2,3,6). However, some organisms have C-1 oxidation pathways for energy production, but lack pathways for the net synthesis of biomass from C-1 precursors (1).

Ruegeria pomeroyi is a member of the roseobacter clade of marine bacteria. This group of organism is highly abundant in coastal water systems (10).

R. pomeroyi was found to lack a robust C-1 pathway when grown on DMSP [see chapter 3]. However, results herein suggest the potential for growth on C-1 compound. Previous studies have shown the ability for bacteria to utilize TRIS buffer as a potential carbon source (5). It is unclear if *R. pomeroyi* is merely deriving energy from C-1 metabolism and utilizing the organic buffer HEPES as a carbon source or if it is consuming the C-1 compounds for both energy and cellular carbon. Future work is necessary to elucidate the mechanism of C-1 metabolism in *Ruegeria pomeroyi*.

4.2 Materials and Methods

Generation of SPO0370 Mutant

Targeted gene replacement of SPO0370 was made by introduction of tetAR by homologous recombination of a suicide plasmid. Up and downstream regions of homology 1000-1500 bp in length and the tetAR genes from pRK415 were PCR amplified and cloned into the pCR2.1 vector by SLIC cloning (8). Plasmid DNA was methylated by CpG methyltransferase as recommended by New England Biolabs and then introduced into R. pomeroyi DSS-3 cells by electroporation. Mutants were selected for ability to grow on tetracycline but not kanamycin, and confirmed by PCR.

Media preparation

Marine basal media (MBM) was prepared as described in Henrisken, 2008 (7).

Growth curves

Three mL cultures of wild-type R. pomeroyi DSS-3 and mutant strains were grown in MBM with 4 mM DMSP or MMPA; 25mM methylamine, trimethylamine or methanol as the sole source of carbon. Acetate and formate were added to a concentration of 6mM. Growth was recorded at an optical density of 600 nm.

4.3 Results

Ethylmalonyl-CoA pathway for acetate and MMPA metabolism

To fully understand growth of *R. pomeroyi* on DMSP, it is also important to know how carbon is metabolized during the demethylation pathway. Previously, the demethylation pathway was

found to form acetaldehyde (9). Because cell extracts contained high specific activities of acetaldehyde dehydrogenase, acetate was hypothesized to be the first common intermediate of central metabolism. *R. pomeroyi* does not possess an ortholog of isocitrate lyase. Thus, this organism appears to be incapable of metabolizing acetate through the glyoxylate cycle. However, *R. pomeroyi* possesses homologs for all known genes in the ethylmalonyl-CoA pathway, which is an alternative means for acetate metabolism. To confirm that the ethylmalonyl-CoA pathway was required for growth on acetate and MMPA, a mutation in the *ccr* gene (SPO0370) was constructed. This gene encodes the crotonyl-CoA carboxylase/reductase enzyme, which is indicative of the ethylmalonyl-CoA pathway (4). The mutant strain was unable to grow on acetate as the sole source of carbon (Figure 1), confirming that acetate was metabolized through the ethylmalonyl-CoA pathway. When MMPA was provided as the sole source of carbon, the mutant displayed an extended lag phase, and the growth yield was diminished by two-thirds (Figure 1). This result was unexpected, as growth on MMPA was expected to behave the same as acetate. In other experiments, slow growth of the wild type was supported by trimethylamine and other C-1 compounds (Figure 2). Currently, it is not known if *R. pomeroyi* is able to grow with C-1 compounds as sole carbon sources. While many of the genes for oxidation of C-1 compounds can be identified in the genome, the presence of the genes for formaldehyde assimilation that are required for growth on these compounds as sole carbon sources are difficult to confirm bioinformatically. An alternative is that the organic HEPES buffer in the medium served as a carbon source and the C-1 compounds served as electron donors under these conditions. If this were true, growth of the *ccr* mutant on MMPA would be primarily supported by oxidation of the methanethiol derived from MMPA and carbon from HEPES. While it is not possible to choose between these explanations at this time, the

severe growth phenotype of the *ccr* mutant provided strong evidence for the role of the ethylmalonyl-CoA pathway in metabolism of carbon from DMSP demethylation. In contrast to the poor growth on MMPA, the mutant was able to grow on DMSP as the sole source of carbon, demonstrating that the cleavage pathway was still functional. These results also indicated that the product of the cleavage pathway does not enter central carbon metabolism as acetate, which was consistent with the acrylate pathway.

4.4 Reference:

1. **Bicknell B., Owens J.D.** 1980. Utilization of methylamines as nitrogen sources by non-methylotrophs. *J Gen Microbiol* 117: 89–96.
2. **Chistoserdova L, Vorholt J.A., Thauer R.K., Lidstrom M.E.** 1998. C1 transfer enzymes and coenzymes linking methylotrophic bacteria and methanogenic Archaea. *Science* 281: 99–102.
3. **Chistoserdova L, Chen S.W., Lapidus A, Lidstrom M.E.** 2003. Methylotrophy in *Methylobacterium extorquens* AM1 from a genomic point of view. *J Bacteriol* 185: 2980–2987.
4. **Erb, T.J., I. Berg A., Brecht V., Muller M., Fuchs G., and Alber B.E.** 2007. Synthesis Of C-5-dicarboxylic acids from C-2-units involving crotonyl-CoA carboxylase/reductase: The ethylmalonyl-CoA pathway. *P Natl Acad Sci* USA 104:10631-10636.
5. **Fabregas, J., Vazquez, V., Cabezas, B., and Otero, A.** 1993. TRIS not only controls the pH in microalgal cultures, but also feeds bacteria. *J. Appl. Phycol*. 5:543–5.
6. **Giovannoni, S.J., Hayakawa, D.H., Tripp, H.J., Stingl, U., Givan S.A., et al**. 2008. The small genome of an abundant coastal ocean methylotroph. *Environ Microbiol* 10: 1771–1782.
7. **Henriksen, J.R.** 2008. Physiology of dimethylsulfoniopropionate metabolism in a model marine Roseobacter, *Silicibacter pomeroyi.* University of Georgia, Athens.

8. **Li, M.Z. and Elledge, S.J.** 2007. Harnessing homologous recombination in vitro to generate recombinant DNA via SLIC. *Nat. Methods* 4:251-256.

9. **Roberts, R.B.** 1955. Studies of biosynthesis in *Escherichia coli*. Carnegie Institution of Washington, Washington,.

10. **Wagner-Döbler, I., & Biebl, H**. 2006. Environmental biology of the marine roseobacter lineage. *Microbiology*, 60(1), 255.

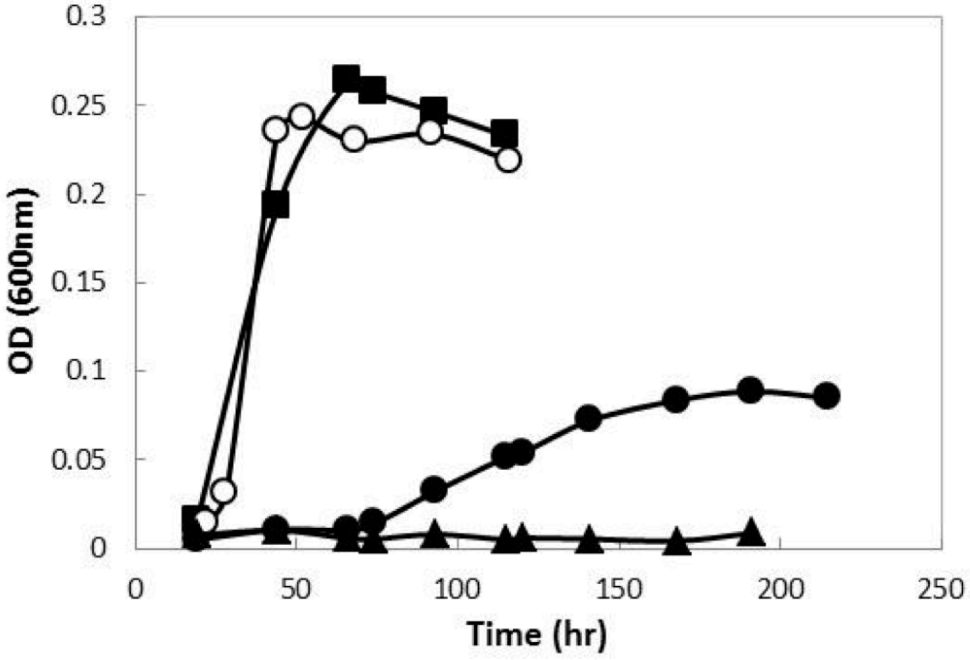

Figure 4.1. Growth of wild-type *R. pomeroyi* and *ccr*$^{-}$ (SPO0370::*tet*). Growth of wild-type cells with 3 mM DMSP (○), 3 mM MMPA (Δ), and 5 mM acetate (□). Growth of *ccr*$^{-}$ with 3 mM DMSP (●), MMPA (▲), and 5 mM acetate (■).

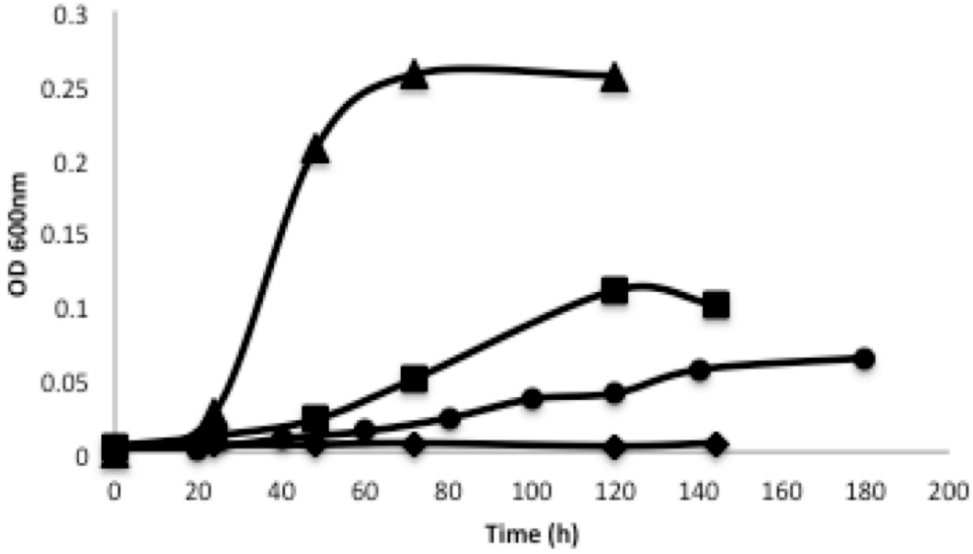

Figure 4.2. Growth of the wild-type cells with 10 mM Formate (●); 25 mM methylamine (■) trimethylamine (▲) and methanol (◆).

APPENDICES

A. Isotope labeled DMSP Synthesis protocol

Preparation of ^{35}S and ^{13}C labeled dimethylsulfide to be used in the synthesis of DMSP.

100mg of elemental ^{35}S (Sigma-Aldrich) was added to the small bottle of a sealed double bottle connected via a side arm. To the small bottle, 5 mL of 0.5M NaOH containing 1g of dithiothreitol was added. The mixture was heated to 120°C in a sand bath until all of the sulfur had dissolved. After cooling, 10mL of 1M HCL was added to the solution to volatilize the reduced ^{35}S. 5mL of 0.5M NaOH was added via syringe to the larger bottle containing a stir bar. The apparatus was positioned to allow stirring overnight to trap the volatilized sulfur in NaOH. After trapping, the solution was removed by syringe and added to a 50 mL round bottom flask. Sulfide concentration was determined upon reaction of DTNB (Ellman's reagent) and an extinction coefficient of ε_{412} = 14.15 mM^{-1} cm^{-1} was used for calculations. The stoppered flask was incubated in an ice bath for 30 min after which time, [^{13}C] methyl iodide was added at a concentration approximately 2 times the molar concentration of the sulfide. Mixture was vigorous stirred for 4 hours under ice bath conditions. After stirring, 1 mL of 2.5M NaOH soln. and 1mL of 0.1M $Na_2S_20_3$ soln. were added to stop the reaction. The flask was connected to a receiving flask of the same dimensions via a U-shaped glass tube to give a closed system. The receiving glass was cooled with dry ice while the mixture was allowed to warm to room temperature. After 2 hours the receiving flask containing the condensed [^{13}C][^{35}S]DMS was removed and stoppered. This labeled DMS was utilized in the standard DMSP synthesis protocol outlined

by Henrisken 2008 (1) adjusting acrylic acid addition for synthesized DMS concentration. The final product formed is a small amount of crystallized DMSP, however, the yield is often very low and synthesis is not consistent. This protocol will need to be improved to generate better yields and consistency.

1. **Henriksen, J.R.** 2008. Physiology of dimethylsulfoniopropionate metabolism in a model marine Roseobacter, *Silicibacter pomeroyi.* University of Georgia, Athens.